

1-1-1976

The feasibility of uranium enrichment with a plasma centrifuge

James Edward Breson
Iowa State University

Follow this and additional works at: <https://lib.dr.iastate.edu/rtd>

 Part of the [Engineering Commons](#)

Recommended Citation

Breson, James Edward, "The feasibility of uranium enrichment with a plasma centrifuge" (1976). *Retrospective Theses and Dissertations*. 17963.

<https://lib.dr.iastate.edu/rtd/17963>

This Thesis is brought to you for free and open access by the Iowa State University Capstones, Theses and Dissertations at Iowa State University Digital Repository. It has been accepted for inclusion in Retrospective Theses and Dissertations by an authorized administrator of Iowa State University Digital Repository. For more information, please contact digirep@iastate.edu.

The feasibility of uranium enrichment
with a plasma centrifuge

by

James Edward Breson

A Thesis Submitted to the
Graduate Faculty in Partial Fulfillment of
The Requirements for the Degree of
MASTER OF SCIENCE

Department: Chemical Engineering and Nuclear Engineering
Major: Nuclear Engineering

Signatures have been redacted for privacy

Iowa State University
Ames, Iowa

1976

TABLE OF CONTENTS

	<u>Page</u>
LIST OF FIGURES	iv
LIST OF TABLES	vi
ABSTRACT	vii
FOREWORD	viii
CHAPTER 1. INTRODUCTION	1
CHAPTER 2. ISOTOPE SEPARATION METHODS	3
Gaseous Diffusion	3
Gas Centrifuge	4
Calutron	7
Plasma Centrifuge	9
Laser Separation	13
Nozzle Separation	13
CHAPTER 3. LITERATURE REVIEW	15
CHAPTER 4. PLASMA CENTRIFUGE ANALYSIS	19
Plasma Centrifuge Model	19
Assumptions	23
Neutral Gas Analysis	24
Plasma Analysis	28
CHAPTER 5. PLASMA CENTRIFUGE FEASIBILITY	32
Process Factor	34
Plasma velocity distribution	34
Configuration	38
Plasma parameters	43
Process factor	49
Mass Flow Rate	52

Power Consumption	73
CHAPTER 6. PLASMA CENTRIFUGE LIMITATIONS	79
Gas Limitations	80
Velocity limitations	80
Mixing	81
Device Limitations	83
Feed injection	83
Product extraction	84
Plasma expansion	85
Wall limitations	86
Shock formation	87
Operating procedures	89
Cascade construction	91
CHAPTER 7. FUTURE WORK	93
Measurement of Parameters	93
Plasma limitations	93
Coupling requirements	94
Plasma velocity profile	94
Temperature distribution	95
Shock formation	95
Pressure variation	96
Design Analysis	96
Optimization	96
Extraction study	97
Three-dimensional study	97
Flow constraints	98
Wall configuration	98
Mode of operation	99
Cascade configuration	100
Economic analysis	100
CHAPTER 8. CONCLUSION	101
REFERENCES	105
ACKNOWLEDGMENTS	107
APPENDIX A. PROGRAM LISTING	108
APPENDIX B. SUPPLEMENTAL FIGURES	116

LIST OF FIGURES

<u>Figure</u>	<u>Page</u>
2.1 Concurrent gas centrifuge.	6
2.2 Electromagnetic process.	8
2.3 Plasma centrifuge.	10
4.1 Experimental plasma centrifuge device.	20
4.2 Plasma centrifuge configuration.	22
5.1 Velocity distribution	37
5.2 Process factor as a function of velocity distribution.	39
5.3 Process factor versus distance, where $\Omega = \text{const.}$	44
5.4 Process factor versus distance, where $\Omega \times r = \text{const.}$	45
5.5 Process factor versus distance, where $\Omega \times r^2 = \text{const.}$	46
5.6 Process factor as a function of angular velocity, where $\Omega = \text{const.}$	48
5.7 Pressure ratio as a function of angular velocity, where $\Omega = \text{const.}$	51
5.8 Table of enriching services.	60
5.9 Enrichment as a function of temperature.	65
6.1 Attached and detached shock.	88
6.2 Turbulence following an obstruction in a superior flow pattern.	90
B.1 Process factor as a function of angular velocity, where $\Omega \times r = \text{const.}$	117
B.2 Process factor as a function of angular velocity, where $\Omega \times r^2 = \text{const.}$	118

- B.3 Pressure ratio as a function of angular velocity, where
 $\Omega \times r = \text{const.}$ 119
- B.4 Pressure ratio as a function of angular velocity, where
 $\Omega \times r^2 = \text{const.}$ 120

LIST OF TABLES

<u>Table</u>	<u>Page</u>
5.1 Spatial distribution, $\omega = \text{constant}$	40
5.2 Spatial distribution, $\omega \times \text{radius} = \text{constant}$	41
5.3 Spatial distribution, $\omega \times (\text{radius})^2 = \text{constant}$	42
5.4 Angular velocity distribution, $\omega = \text{constant}$	47
5.5 Temperature distribution, $\omega = \text{constant}$	50
5.6 Velocity produced wall limitations	53
5.7 Temperature produced wall limitations	54
B.1 Angular velocity distribution, $\omega \times \text{radius} = \text{constant}$	121
B.2 Angular velocity distribution, $\omega \times (\text{radius})^2 = \text{constant}$	122
B.3 Temperature distribution, $\omega \times \text{radius} = \text{constant}$	123
B.4 Temperature distribution, $\omega \times (\text{radius})^2 = \text{constant}$	124

ABSTRACT

The plasma centrifuge is an enrichment device that uses an electromagnetic force to drive a partially ionized plasma and subsequently the surrounding neutral gas. Theoretically, the device offers a number of advantages over competing enrichment schemes; including no mechanical moving parts, high separation, and low wall interactions. The neutral gas in the plasma centrifuge may be analyzed as two gas regions and a plasma region, with the gas obeying the Navier-Stokes equation in the gas regions and the gas conforming to the plasma velocity distribution in the plasma region. The device predicts a process factor of 1.20 with a mass flow rate of about 45 kg/year. The energy consumption should be competitive with the gaseous diffusion and gas centrifuge technique. The device should not be restricted by problems with shock waves, mixing, or instabilities. The primary limitation will be due to the inability to deplete the feed. Additional studies are needed to predict plasma distributions, device parameters, and gas behavior.

This analysis predicts that the plasma centrifuge will produce high enrichment for any plasma velocity distribution. Since the gas is only slightly depleted at the inner wall, an ideal cascade cannot be constructed, reducing the separative power and increasing the number of stages. Although the plasma centrifuge appears feasible for enrichment, the low depletion factor makes construction of a traditional cascade impractical.

FOREWORD

The development of a viable enrichment scheme is a detailed process. The stages in the development program range from the initial analytical predictions, to component testing, to the complete cascade construction. The development of the plasma centrifuge is still in the initial stages, analysis of the feasibility and parameter measurements on experimental devices.

This study will continue the analysis work by considering the most promising plasma centrifuge application; a neutral gas that is placed in rotation by the crossed electric and magnetic fields that drive a rotating, partially ionized plasma. The analysis treats the neutral gas as an inviscid fluid in the regions where the plasma-neutral gas coupling is weak, and treats the neutral gas by the distributions that govern the plasma in the region where the plasma-neutral gas coupling is strong.

The plasma and neutral gas will be coupled in regions where the difference between the plasma and gas velocity is much less than the plasma velocity. This condition will be met for specific values of the plasma density, neutral gas density, temperature, and device dimensions. These parameters may all be determined except for the plasma density distribution. To proceed with the analysis, either a specific density distribution must be assumed, or specific coupling locations must be assumed. The latter assumption is used in this analysis since it permits a more general solution and retains the largest number of degrees of freedom, including the initial gas density,

degree of ionization, temperature, and magnitude of the electric and magnetic fields.

The technique permits the prediction of the maximum flow of enriched material with the only constraints being the parameters required for maintenance of the rotating plasma. The analysis also permits optimization studies of optimization trends.

After the feasibility analysis has been completed, the device must be analyzed for potential problems and limitations. The problems will indicate physical constraints that may be encountered, such as the formation of a shock wave or the limitations of a cascade. Analyzing the limitations of an enrichment technique produces a number of results. The analysis permits design modification to produce a more efficient device. The analysis generates new information and identifies areas requiring additional research. And the analysis identifies specific problems that could ultimately make the technique infeasible.

An analysis of this type studies what the device can ultimately produce, what efficiency the device will currently operate at, and what problems must be solved to produce a viable enrichment scheme.

CHAPTER 1. INTRODUCTION

The future of nuclear power relies, at least in part, on the continued supply of slightly enriched uranium. The present generation of nuclear power plants requires the use of uranium enriched to a level of 2-4% ^{235}U . This enrichment is currently provided by the gaseous diffusion technique, but this situation may change in the near future. Advances in enrichment techniques, notably the gas centrifuge and laser separation technique, may provide the same enrichment at a much lower cost [1, 2]. The gas centrifuge and laser separation method may provide high separation factors, reducing the number of stages and capital cost. In addition, the energy consumption in these devices is estimated to be only 10% of the energy consumed in the gaseous diffusion process [1].

The high capital cost and high operating cost has spurred interest not only in the gas centrifuge and laser separation, but also in more advanced techniques such as the plasma centrifuge process.

Since the two naturally occurring isotopes of uranium display the same chemical properties, the separation process must make use of the mass difference. The difference in the atomic mass between the two isotopes can be used to produce a different property, such as the radius of rotation in the centrifuge, or to produce a difference in the ionization state, as in the laser separation method. When the two isotopes become physically distinct, the product can be extracted by mechanical or electrical separation processes.

In Chapter 2, the basic features of the different separation schemes are discussed with respect to the principle of operation, the actual or expected separation factor, mass flow rate, major advantages, and limitations. Chapter 3 considers the current research on the plasma centrifuge technique. Chapter 4 describes the model used in the analysis of the plasma centrifuge. In Chapter 5, the feasibility of the plasma centrifuge is considered. Particular emphasis is placed on the separation factor, mass flow rate, pressure limits, gas density limitations, and energy consumption. The major limitations of the plasma centrifuge are discussed in Chapter 6. Chapter 7 considers the direction of future research needed to further evaluate the feasibility of the plasma centrifuge.

CHAPTER 2. ISOTOPE SEPARATION METHODS

To evaluate the feasibility of the plasma centrifuge, the device must be compared with the competing enrichment methods. To facilitate this comparison, a brief description of each device follows. In addition, the major advantages and limitations are listed.

Gaseous Diffusion

The need for uranium enrichment arose during the early stages in the weapons program during World War II. The gaseous diffusion technique was selected for the government enrichment plants because of the system reliability and proven technology.

The operation of the gaseous diffusion plant is based on the principle of molecular effusion. The uranium in this technique is in the form of uranium hexafluoride (UF_6), a gas at room temperature. The lighter molecules in the mixture, the molecules containing atoms of ^{235}U , strike the walls of the container more frequently than the heavier molecules [1]. The container walls in the diffusion plant are perforated by small holes. Since the lighter gas strikes the wall more frequently, the gas escaping the container will be slightly enriched in the lighter fraction, $^{235}UF_6$. The theoretical maximum process factor in this case is given by $(M_2/M_1)^{1/2} - 1$. The maximum process factor in this case is 1.0043, so that the diffused gas will contain 1.0043 times as much $^{235}UF_6$ as the feed gas.

The gaseous diffusion plants are the mainstay for world uranium enrichment. The advantages of the technique are the same now as in

1942; the concept is well understood and the technology is already proven. The disadvantages are due to high cost and energy consumption. The process factor is low, so that a large number of stages must be used. Since natural uranium contains only 0.711% ^{235}U , the gaseous diffusion plants require 2100 to 3300 stages to enrich the uranium to 2-4% ^{235}U . The process is also highly energy intensive. To maintain a high mass flow rate, the feed gas must be kept at a high pressure, requiring a large electric load to the system compressors. Coupled with the low process factor and large number of stages, the gaseous diffusion technique becomes highly energy intensive. Diffusion plants now require about 3100 kWhr/(kg SWU) [2], while centrifuge plants may require only about 300 kWhr/kg SWU, which should permit the centrifuge plants to produce slightly enriched uranium at a lower cost than the diffusion plants, where Separative Work Unit is denoted by SWU.

Gas Centrifuge

The gas centrifuge offers several advantages over the gaseous diffusion technique. Avery and Davies predict that the centrifuge will produce higher process factors, reducing both the number of cascades and energy requirements [1]. The separation process factor for this device is related to ΔM , rather than $(M_2/M_1)^{1/2} - 1$. A gas centrifuge operating with a peripheral velocity of 300 m/sec would yield a process factor of 1.055. To evaluate the improvement of this device over the diffusion plant, consider the simple process difference, ϵ , where $\epsilon = 1$ - simple process factor. The diffusion plant has a

process difference of 0.055, a value nearly 13 times higher. The technique shows an obvious reduction in the number of stages, and ultimately in the energy requirement, producing slightly enriched uranium at a lower cost than from the diffusion plants.

The gas centrifuge operates by creating pseudo-gravitational forces in a UF_6 gas, causing separation of two components due to the mass difference between the two uranium isotopes. The uranium hexafluoride gas is placed in rotation by mechanically rotating the cylindrical confinement chamber. The centrifugal forces on the rotating gas cause the heavy fraction to diffuse to the outside of the cylinder while the lighter fraction is driven to the inside. Figure 2.1 is an example of a concurrent gas centrifuge [1]. The gas entering at the bottom of the figure could be either natural feed or the output from an earlier enrichment stage. The rotor is mechanically rotated, placing the gas in rotation. The mass difference causes the gas to split into two fluids that rotate with different radii (shown as a_1 and a_2). The exit at the top of the figure shows the channels for the two gas fractions.

The gas centrifuge offers several advantages over the gaseous diffusion plant. The higher process factor permits enrichment with fewer stages, permitting a reduction in the capital investment. A higher mass flow rate is possible since the centrifuge process is a flow system, whereas the diffusion plants rely on molecular effusion. The gas need not be maintained at such a high pressure to ensure acceptable flow rates, which reduces the compressor load found in the diffusion plants. Coupled with the smaller number of stages, the

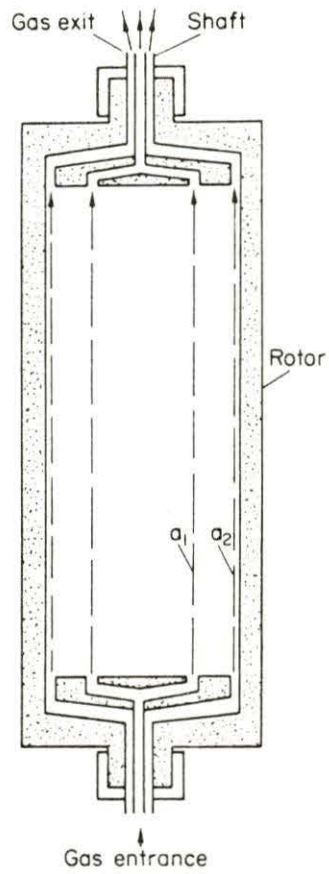


Fig. 2.1. Concurrent gas centrifuge [1].

electrical load is significantly reduced. Avery and Davies estimate that the centrifuge plants will consume only one tenth the energy required by the diffusion plants [1].

The centrifuge also has a number of limitations. The concept was abandoned during the weapons program because of unacceptably high losses in the bearings of the rotor. Although advances in both materials and design have permitted operation, the system is still limited by these losses. The rotor can only attain a peripheral velocity of about 400 m/sec, effectively limiting the process factor. The system must also display stable rotation to prevent mixing of the gas streams. The gas centrifuge is also limited by wall interactions. The uranium hexafluoride gas is highly corrosive. With the centrifuge, the point of maximum shear is the inner wall edge, since here the slower moving gas collides with the rapidly rotating wall of the cylinder. The interactions create wall deterioration and contamination.

The advantages of the gas centrifuge seem to outweigh the disadvantages. It appears that the next generation of enrichment plants will employ the gas centrifuge technique.

Calutron

The calutron is the third type of isotope separator to be considered. The calutron employs the electromagnetic process. Figure 2.2 is an example of such a device [1].

Ionized atoms pass through the slits where they encounter a magnetic field. The force on the particles is given by the equation

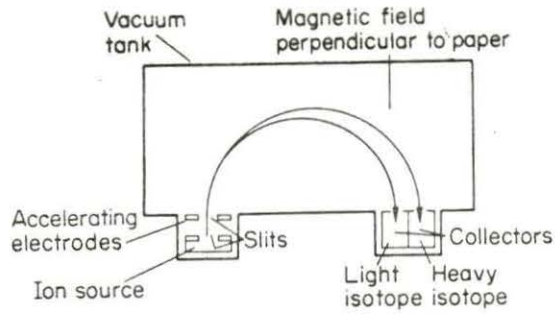


Fig. 2.2. Electromagnetic process [1].

$$\vec{F} = q\vec{V} \times \vec{B} \quad (2.1)$$

where q = charge of the particle

\vec{V} = velocity vector of the particle

\vec{B} = magnetic field.

The force is in turn given by, $F = mv^2/r$. If the particles enter with the same velocity, are ionized to the same degree, and see a homogeneous magnetic field, the radius of the trajectory will be proportional to the mass of the ion. The light isotope will take a trajectory with a smaller radius, permitting separation of the two isotopes.

The calutron offers a number of advantages. The system is well understood and operating technology exists. The process, in principle, should produce large separation factors, permitting slightly enriched uranium to be produced in a single stage. Unfortunately, the calutron also has a number of limitations. The system is limited to low flow rates due to the difficulty of producing a large flow of ions. The calutron is also limited by a spread in the velocity of the incoming ions. The ions must have the same velocity to produce good resolution at the collection points. In addition, the calutron displays problems

with space charge effects, beam focusing, resolution, and particle neutralization.

The calutron is not acceptable for industrial use due to these problems. Because of the high process factor, the method is valuable for high enrichment uses, but not to produce slightly enriched uranium.

Plasma Centrifuge

The plasma centrifuge may be considered to be a hybrid between the gas centrifuge and the calutron. The device operates on the same principle as the gas centrifuge, the pseudo-gravitational forces are created in the rotating gas. The driving force in this case is the crossed electric and magnetic fields, rather than the rotating mechanical cylinder. The device offers the ease of control and high process factors of the calutron, while eliminating the mechanical and material limitations of the gas centrifuge.

The plasma is created by discharging a set of capacitors through the neutral gas in the presence of an axial magnetic field and radial electric field. The initial discharge causes a small amount of ionization. The charged particles are contained by the magnetic field and begin to rotate in the presence of the crossed electric and magnetic field. The $\vec{E} \times \vec{B}$ force drives the charged particles to higher velocities, resulting in further ionization when the charged particles strike the slower moving neutral particles. The degree of ionization depends initially on the magnitude of the discharge, and finally on the crossed electric and magnetic field strength as well as the plasma temperature

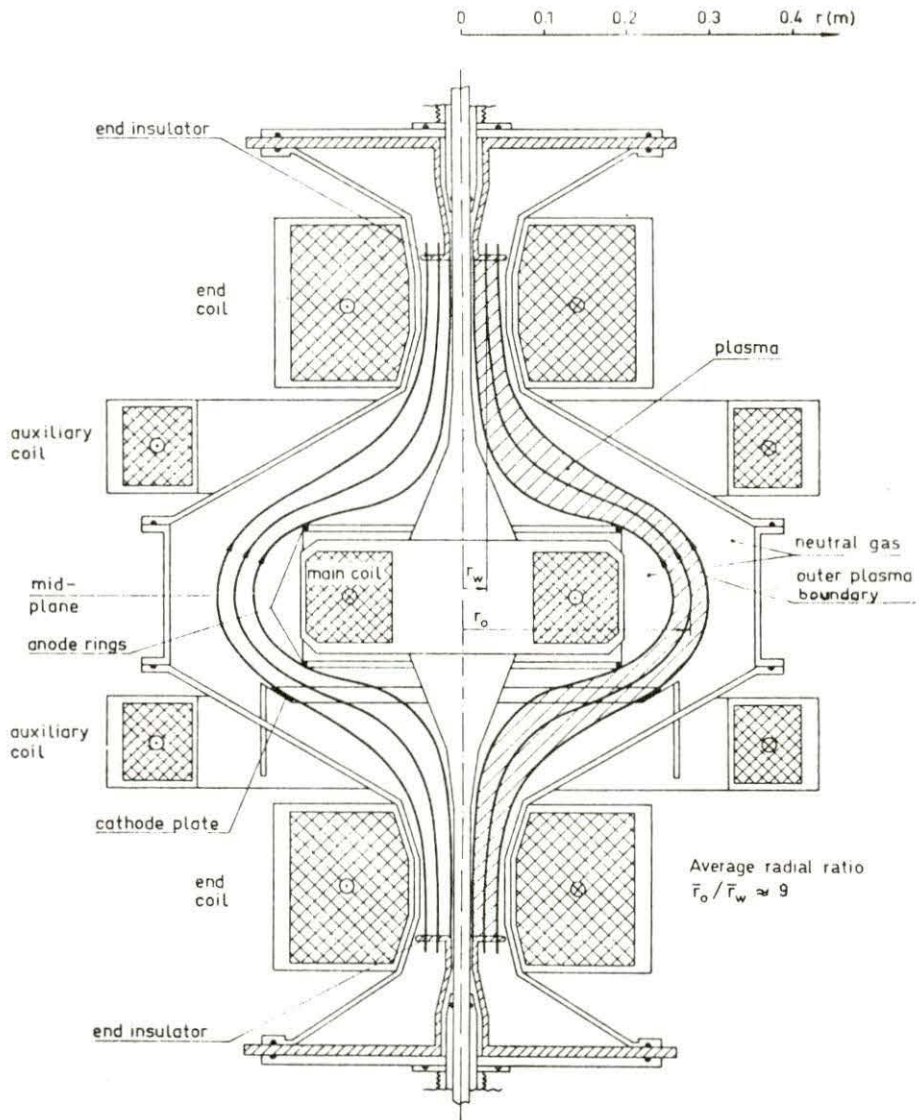


Fig. 2.3. Plasma centrifuge [3].

and density [4]. The plasma is then a collection of mobile positive and negative charged particles contained by the magnetic field [5].

The plasma temperature and density are lower than those required for thermonuclear applications. The ionized gas is only a small fraction of the original gas. The neutral particles will exert a drag force on the rotating charged particles. The crossed electric and magnetic fields continue to drive the ionized particles, and the same drag force eventually places the neutral gas in rotation [6].

The system is analogous to the gas centrifuge, the driving force in this instance being the crossed electric and magnetic field rather than the mechanical rotor. As in the gas centrifuge, the heavier elements will be driven to the outer wall while the lighter elements are driven to the inner wall, provided that the degree of ionization is the same for the elements. This physical separation again permits extraction of a product stream.

The plasma centrifuge offers a number of distinct advantages. The rotating plasma has been used extensively for fusion research. The operation is understood and the technology exists to produce devices at the temperature and density desired [4]. Since the plasma temperature and pressure are much lower than thermonuclear applications, the confining magnetic field requirements are much lower and may be met by present day technology. The device offers several other advantages over both the gaseous diffusion method and gas centrifuge [7, 8]:

- 1) No moving mechanical parts, since the motion is controlled by the electric and magnetic fields

- 2) Higher velocities are attainable than with the gas centrifuge
- 3) Complete external control by means of the crossed electric and magnetic fields
- 4) Stable velocity profiles
- 5) Reduced material constraints due to decreased interactions between the containment wall and neutral gas
- 6) Low power consumption due to the low ionization degree
- 7) High process factor
- 8) High mass flow rates.

The plasma centrifuge also has a number of limitations, several of which will be analyzed in Chapter 6. The plasma centrifuge is subject to instabilities due to velocity differences, temperature profiles, feed material injection, and product extraction. Mixing may eliminate the separation effect. The system is limited in either size or velocity by flow rate considerations and pressure gradients, since the enriched uranium must be extracted from the low density gas at the inner wall. Flow is limited in the axial direction since the gas requires time to separate. Finally, the plasma centrifuge is limited now by inadequate information concerning system parameters; including temperature profiles across the gas and plasma, velocity profiles in the gas and plasma, and gas behavior in high temperature, low density applications.

Laser Separation

The laser separation process is one of the most promising of the advanced enrichment schemes. The process also employs the difference in masses for the two isotopes, or more specifically, the differences in ionization potential. Although the uranium isotopes behave the same chemically, they have slightly different ionization potentials, due to the difference in atomic mass. If a laser can be finely tuned to produce a beam of photons of the same energy as that of one of the isotopes, that particular isotope can be preferentially ionized [9]. Once ionized, that isotope may be removed from the gas by a magnetic field, resulting in a higher enrichment of the remaining component.

The laser separation process may provide very high process factors with low energy consumption. The process has had very favorable results in experiments to separate other isotopes [10]. The technique is also susceptible to a number of limitations. The system is still limited by mixing due to removal of the ionized particles. The tuning of the laser is also critical, since a spread in the laser energy will cause ionization of both species, resulting in lower process factors. Lawrence Livermore Laboratory, the Los Alamos Scientific Laboratory, and Exxon Nuclear have active research programs investigating uranium enrichment by the laser separation technique.

Nozzle Separation

The separation nozzle technique is the final method to be considered. Although the nozzle process is not being employed in the United States,

it is considered a viable technique in Europe [2, 11]. The technique combines pressure diffusion and a centrifugal effect to produce the desired separation. A jet of UF_6 gas is expanded through a narrow slit along a curved wall. The wall deflects the jet and causes a partial separation of the species. The heavier fraction of the gas will remain close to the wall while the lighter fraction will assume a trajectory of smaller radius [1]. The two fractions are then separated in space and may be either collected or diverted to additional stages for further enrichment.

The process promises to produce slightly enriched uranium at a lower cost than the diffusion plants due to the lower capital cost and reduced energy consumption. Unfortunately, the process suffers a number of limitations. The UF_6 gas is highly corrosive. The nozzle components must be constructed to exact tolerances to prevent mixing, and hence the corrosion reduces performance. The knife edge that must separate the two fractions suffers the same material limitations. In addition, the edge must be exactly positioned in order to use the small spatial separation produced by the process. Finally, velocity distributions in the jet will produce the same mixing described in the section on the calutron.

CHAPTER 3. LITERATURE REVIEW

Plasma centrifuges were developed in the early sixties to heat plasmas to thermonuclear temperatures. A number of problems, including the critical velocity phenomenon, plasma streaming, and instabilities [4] prevented the plasma temperature in the centrifuge from reaching thermonuclear values.

The plasma centrifuge displays several characteristics that permit industrial applications other than plasma heating. Lehnert shows that the plasma displays high angular velocities and stable velocity profiles [4]. These characteristics make the plasma centrifuge particularly promising as an isotope separation device.

The plasma centrifuge has received attention both in the United States and Sweden. A detailed description of rotating plasmas is given by Lehnert [4]. The devices differ widely with respect to polarity, magnetic field strength, longitudinal length, gas density, and gas type. Examples of plasma centrifuges are shown in Fig. 2.3 and Fig. 4.1. This paper will be limited to the isotope separation applications of rotating plasmas.

The plasma is created by passing an electric field through a neutral gas. The field causes heating and some degree of ionization. For the plasma centrifuge, the gas will be only partially ionized. A large amount of energy is consumed in creating a fully ionized plasma. To create a fully ionized uranium plasma, all 92 electrons must be stripped from each atom. The removal of the first electron requires an energy of 6.08 eV [12], corresponding to a temperature

of over 47,000 K. The operating temperature in a plasma centrifuge will be only 10,000 K, and possibly as low as 2500 K. The low temperature results in a low degree of ionization, with the charged fraction being ionized to the first state. Lehnert [8] and Okada et al. [13] have shown that this degree of ionization is still capable of placing neutral gas in rotation. Since the separation factor is inversely related to temperature, low temperature operation will provide higher process factors. High process factors result in higher enrichment per stage, requiring fewer stages to produce the same enrichment.

Plasma centrifuges have been studied theoretically to analyze uranium isotope separation. An early work by Bonnevier [14] studied the possibility of separation in a fully ionized rotating plasma. He estimates a process factor of 1.134, which is an improvement over the diffusion plant factors of 1.0043 and the gas centrifuge at 1.055. Lehnert [8] analyzed a partially ionized plasma centrifuge. For the configuration that he studied, the process factor was about 1.06. Okada et al. [13] carried a similar analysis in 1973 and concluded that a device could be constructed to produce a process factor of 1.25, enriching natural uranium to 3% ^{235}U in only 13 stages. The difference in these results is attributed to differences in assumptions and parameters used in the analysis. For example, Bonnevier assumed an operating temperature of 200,000 K, Lehnert a temperature of 10,000 K, and Okada et al. a temperature of 2500 K. Other differences in assumptions include device configuration, the assumed velocity profiles, and plasma density assumptions.

Although only theoretical studies have been performed for the uranium isotopes, operating data has been collected on the separation of other elements and isotopes [8, 15], including isotopes of hydrogen, helium, neon, and argon. To date, several problems have prevented separation factor measurements, principally instabilities induced by the probe introduction [15]. The devices are operated on a pulsed basis and are hampered by stability problems [16]. In addition, no adequate method exists to extract the separated element, without disturbing the plasma equilibrium [15]. The instability in this instance is due to probe-plasma interactions.

Present experimental studies concentrate on the understanding of rotating plasma behavior. One particular area of active research is the study of the critical velocity phenomenon. The ions and electrons in a rotating plasma stream along the axial magnetic field lines. The ions and electrons recombine at the end insulators to form neutral particles. The neutral particles form a wall layer at the end insulator and begin to diffuse back into the plasma. The rapidly rotating charged particles strike these diffusing particles, causing ionizations. The charged particles create an electric field that prevents the gas from being driven to a higher velocity than a particular critical velocity. Concentric metal rings [17] and extended radial ratios [3] are being explored as techniques to suppress the phenomenon or to exceed the critical velocity. The research is very important because the centrifuge is limited to a maximum rotational velocity. Suppression of the critical velocity phenomenon would permit plasmas to rotate at higher velocities, producing higher separation factors.

The question of extraction of the separated element is of particular importance. A probe placed in the rotating gas will cause disturbances and mixing that may diminish or even eliminate the separation. Probes placed in the plasma cause even more serious problems. The question of stability itself is important. System oscillations due to transients in electric or magnetic fields, or due to gas insertion and extraction must be considered. Temperature changes cause differences in separation factors and pressure ratios, providing additional transients.

Although work has been performed on rotating plasmas, the work has not widely been applied to isotope separation. Some experimental results have been obtained for other isotopes and elements, but not for uranium enrichment. A feasibility study is clearly needed at this time to study the effect of varying parameters such as temperature, density, and gas dimensions. The theoretical studies have not yet been completed, and surely no experimental results exist.

CHAPTER 4. PLASMA CENTRIFUGE ANALYSIS

An isotope separation device will be practical if it can produce an appreciable quantity of product at a cost competitive with other enrichment methods. This implies the use of a good separation method that can produce a high process factor, a high mass flow rate, small initial investment, low operating cost, or some combination of the above. The demonstration of the feasibility of the enrichment scheme does not suffer the constraints imposed on a demonstration device. This chapter describes the centrifuge model used in this analysis as well as the derivation of the expressions for pressure distributions, particle number density, and enrichment. Chapter 5 discusses the feasibility of the plasma centrifuge and Chapter 6 considers the engineering problems that may be encountered in the construction of a demonstration device.

Plasma Centrifuge Model

The gas centrifuge may be analyzed as three distinct regions. Figure 4.1 shows a schematic diagram of a plasma centrifuge device [18].

The figure shows the three regions in the device. The partially ionized plasma divides the gas into two regions. The volume inside the radius r_{01} will be designated region 1 and termed the inner gas region. The region contained between $r_{01} < r < r_{02}$ will be designated region 2 and termed the plasma region. The region such that $r > r_{02}$ will be designated region 3 and termed the outer gas region.

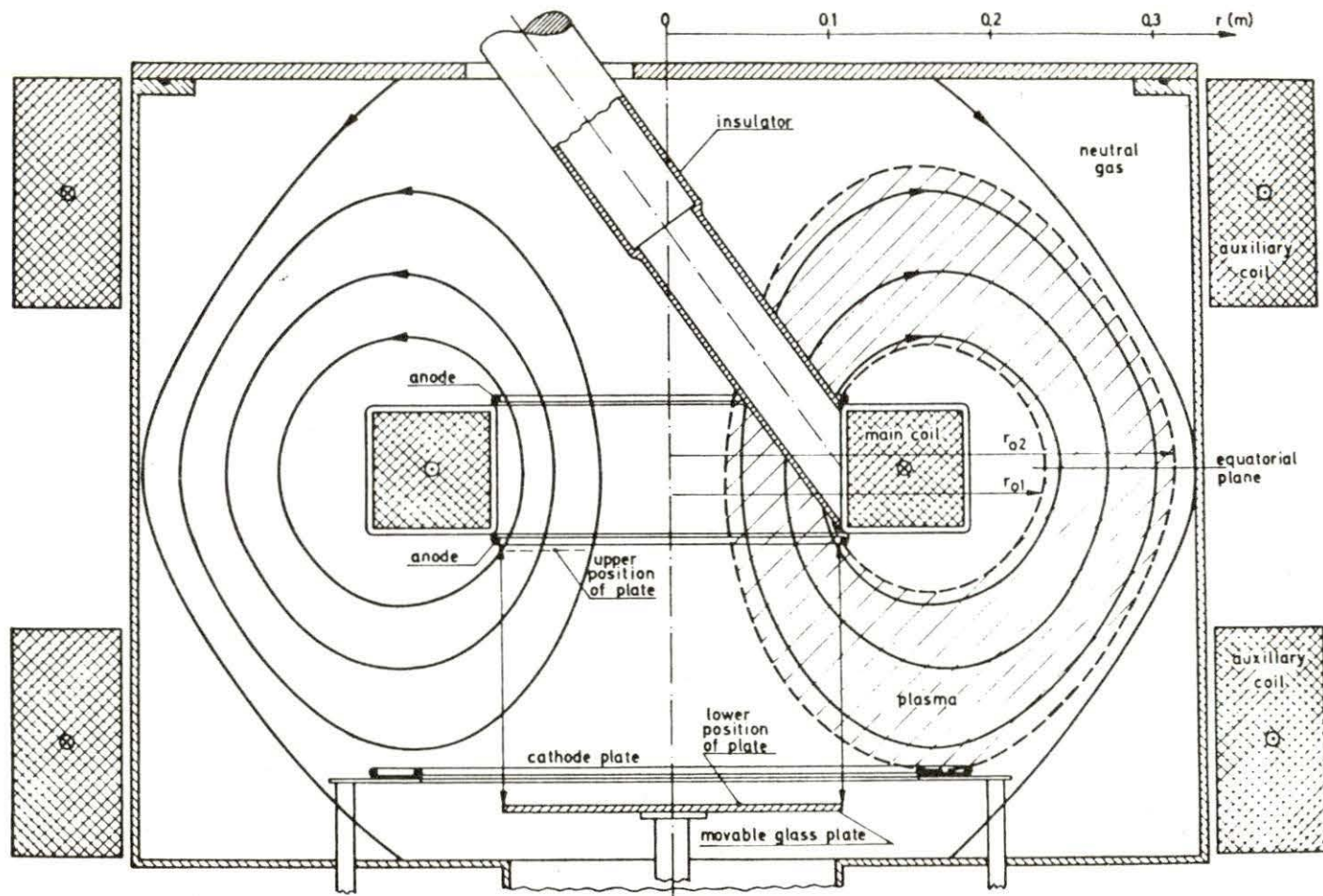
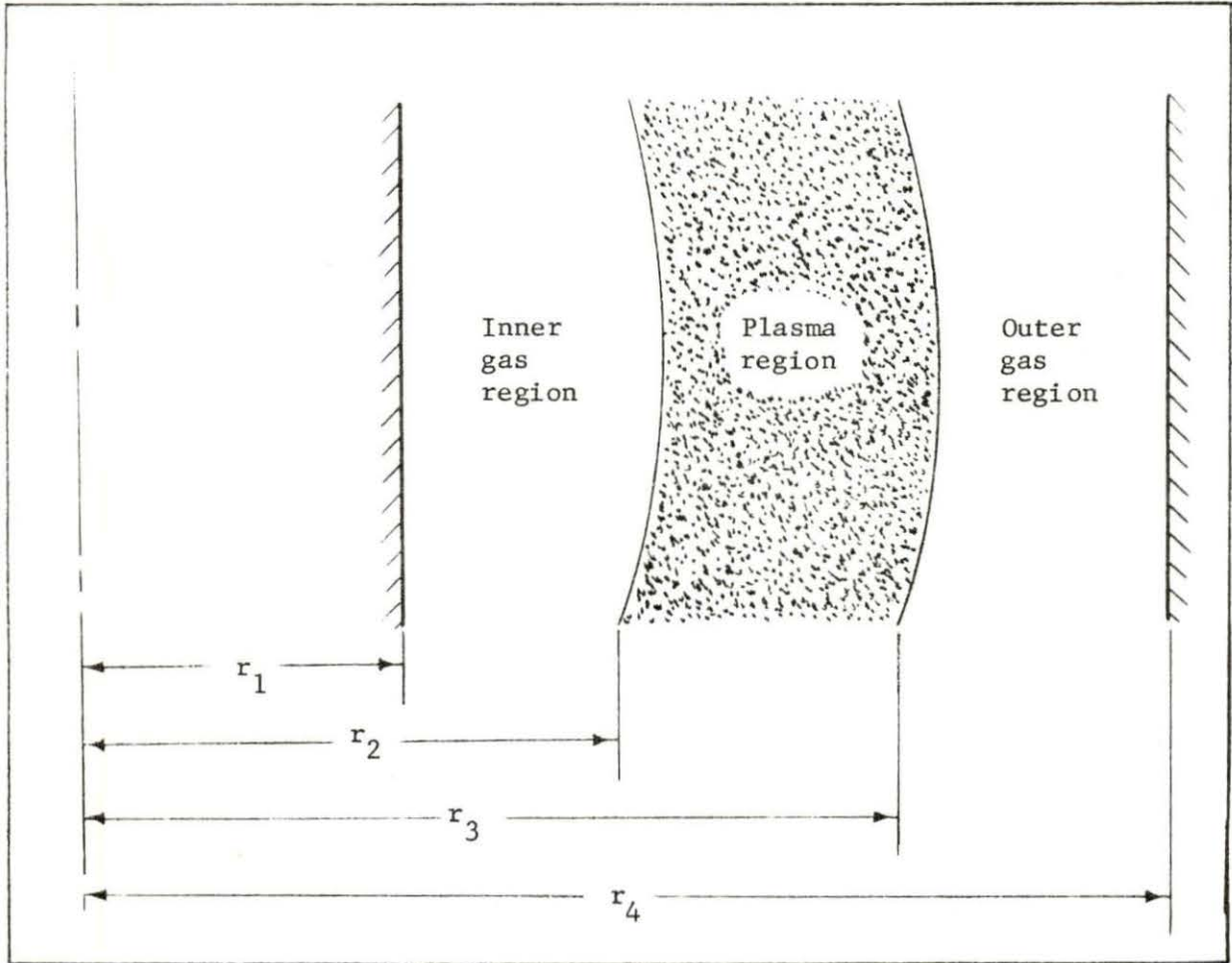


Fig. 4.1. Experimental plasma centrifuge device [18].

The plasma in such a device is only partially ionized. The degree of ionization will be only 1-3% [8, 13]. The majority of particles in the plasma region will be neutral particles, not charged particles. The degree of ionization is low because the device uses a low temperature, low density plasma confined by a magnetic field of low strength. The low temperature produces higher separation factors and the low energy magnetic field reduces the power consumption. Lehnert estimates that the power consumption in such a device is three orders of magnitude lower than the power consumption in a fully ionized plasma [8].

The boundaries for the three regions are not distinct. Since the magnetic field strength is low, charged particles can migrate into the gas regions. Conversely, the outflow of particles is balanced by a back flux of neutral and charged particles to maintain continuity. Neutral particles are also being ionized in the plasma region by collisions with charged particles, as discussed in Chapter 2. The boundaries may be defined by the criteria established by Lehnert [8]. For coupling between the plasma and neutral gas, the differential velocity between the charged particles and the neutral particles must be much lower than the velocity of the charged particles. The coupling is dependent on the device dimensions, particle velocity and particle density. The regions used in this analysis are bounded by the points where the plasma and neutral gas become coupled. Figure 4.2 is an example of such a configuration. If an accurate density distribution was known for the plasma, the boundaries could be accurately defined. As mentioned earlier, this is a field of active research for plasma analysis.



r_1 = Radius of inner wall

r_2 = Radius of inner plasma edge

r_3 = Radius of outer plasma edge

r_4 = Radius of outer wall

Fig. 4.2. Plasma centrifuge configuration.

Assumptions

The following assumptions are made for this analysis:

- 1) The system is in steady state operation
- 2) The plasma is subjected to a homogeneous axial magnetic field and radial electric field
- 3) The plasma pressure is constant in space
- 4) The temperatures of the plasma and neutral gas are assumed constant in space, since physical distributions have not yet been determined
- 5) The ionization degree n/n_n is low, where n is the charged particle density and n_n is the number density of neutral particles
- 6) The neutral gas is effectively coupled to the plasma in the plasma region
- 7) Plasma neutral gas interactions in either of the gas regions are neglected
- 8) The neutral gas velocity in the gas region is governed by the Navier-Stokes equation. Since a gas at this temperature is inviscid, and the static pressure much less than the centrifugal force, the equation

$$\frac{d}{dr} \left(\frac{1}{r} \frac{d(rv_\theta)}{dr} \right) = 0$$
- 9) The rotational velocity of the neutral gas goes to zero at the walls.

Neutral Gas Analysis

The pressure and density of the neutral gas in the inner and outer region can be determined from the gas velocity. The velocity of the gas is given by

$$\frac{d}{dr} \left(\frac{1}{r} \frac{d(rv_{\theta})}{dr} \right) = 0 \quad (4.1)$$

The boundary conditions for the inner gas region are as follows:

- 1) $v_{\theta} = 0$ at r_1
- 2) $v_{\theta} = v_{\theta p}$ at r_2

where

$v_{\theta p}$ = rotational velocity of the charged particles

r_1 = radius of the inner wall

r_2 = radius of the inner plasma boundary.

Rearranging terms,

$$\frac{d^2 v_{\theta}}{dr^2} + \frac{d}{dr} \left(\frac{v_{\theta}}{r} \right) = 0 \quad (4.2)$$

Integrating and applying the two boundary conditions, equation 4.2 is solved to yield

$$v_{\theta i}(r) = \frac{r_2 v_{\theta pi}}{(r_2^2 - r_1^2)} \left[r - \frac{r_1^2}{r} \right] \quad (4.3)$$

where

$v_{\theta i}(r)$ = rotational velocity of neutral gas in the inner
gas region

$v_{\theta pi}$ = rotational velocity of the plasma at the inner gas-
plasma interface

r_1 = radius of the inner wall

r_2 = radius of the neutral gas-plasma interface.

The angular velocity can be easily determined from the rotational velocity by the equation $\omega = v_\theta / r$. Making this substitution

$$n_i(r) = \frac{r_2^2 \omega_{ci}}{(r_2^2 - r_1^2)} \left[1 - \frac{r_1^2}{r^2} \right] \quad (4.4)$$

where

$n_i(r)$ = angular velocity of the inner neutral gas

ω_{ci} = rotational velocity at the inner neutral gas-plasma interface.

The pressure and density distribution can be determined from the following expression [7],

$$\frac{dp}{dr} = nm n^2 r \quad (4.5)$$

where

p = pressure of the gas

n = particle number density of the gas

m = mass of the gas particles.

n = angular velocity of the rotating gas

The pressure is further related by the expression, $p = nkT$. Substituting for n and rearranging

$$\frac{dp}{p} = \frac{n^2 m r dr}{kT} \quad (4.6)$$

The expression for the angular velocity in the inner neutral gas region is given by equation 4.4. Substituting

$$\frac{dp}{p} = \left(\frac{r_2^2 \omega_{ci}}{(r_2^2 - r_1^2)} \left[1 - \frac{r_1^2}{r^2} \right] \right)^2 \frac{mr dr}{kT} \quad (4.7)$$

$$\frac{dp}{p} = \frac{r_2^4 \omega_{ci}^2 m}{(r_2^2 - r_1^2)^2 kT} \left[r - \frac{2r_1^2}{r} + \frac{r_1^4}{r^3} \right] dr \quad (4.8)$$

Solving

$$\ln \left(\frac{p(r)}{p_0} \right) = \frac{\omega_{ci}^2 m r_2^4}{(r_2^2 - r_1^2)^2 kT} \left[\frac{(r^2 - r_1^2)}{2} - 2r_1^2 \ln \left(\frac{r}{r_1} \right) + \frac{r_1^4}{2} \left(\frac{1}{r_1^2} - \frac{1}{r^2} \right) \right] \quad (4.9)$$

where p_0 = gas pressure at the inner wall.

The gas density is given by the same expression.

$$p = nkT \quad (4.10)$$

$$dp = dn(kT) \quad (4.11)$$

Dividing equation 4.11 by equation 4.10,

$$\frac{dp}{p} = \frac{dn}{n} \quad (4.12)$$

The following expression gives the gas density as a function of position r ,

$$\ln \left(\frac{n(r)}{n_0} \right) = \frac{\omega_{ci}^2 m r_2^4}{(r_2^2 - r_1^2)^2 kT} \left[\frac{(r^2 - r_1^2)}{2} - 2r_1^2 \ln \left(\frac{r}{r_1} \right) + \frac{r_1^4}{2} \left(\frac{1}{r_1^2} - \frac{1}{r^2} \right) \right] \quad (4.13)$$

The expression for the outer neutral gas region can be obtained in a similar manner

$$v_{\theta 0}(r) = \frac{r_1 v_{\theta p 0}}{(r_2^2 - r_1^2)} \left[\frac{r_2^2}{r} - r \right] \quad (4.14)$$

where

$v_{\theta 0}(r)$ = rotational velocity of the outer neutral gas

$v_{\theta p 0}$ = rotational velocity at the plasma-outer gas interface

r_1 = radius of the plasma-outer gas interface

r_2 = radius of the outer wall.

$$n_0(r) = \frac{r_1^2 \omega_{c0}}{(r_2^2 - r_1^2)^2} \left[\frac{r_2^2}{r^2} - 1 \right] \quad (4.15)$$

where

$n_0(r)$ = angular velocity of the outer gas

ω_{c0} = angular velocity at the plasma-outer gas interface.

$$\ln\left(\frac{p(r)}{p_0}\right) = \frac{r_1^4 \omega_{c0}^2 m}{(r_2^2 - r_1^2)^2 kT} \left[\frac{(r^2 - r_1^2)}{2} - 2r_2^2 \ln\left(\frac{r}{r_1}\right) + \frac{r_2^4}{2} \left(\frac{1}{r_1^2} - \frac{1}{r^2}\right) \right] \quad (4.16)$$

$$\ln\left(\frac{n(r)}{n_0}\right) = \frac{r_1^4 \omega_{c0}^2 m}{(r_2^2 - r_1^2)^2 kT} \left[\frac{(r^2 - r_1^2)}{2} - 2r_2^2 \ln\left(\frac{r}{r_1}\right) + \frac{r_2^4}{2} \left(\frac{1}{r_1^2} - \frac{1}{r^2}\right) \right] \quad (4.17)$$

From the pressure distribution, the pressure or density at any point can be determined. The density ratio may be numerically integrated across the configuration. From the total number of particles in the device, the wall pressure and density can be determined, and the pressure expression gives the neutral gas pressure or density at any point in the device.

Plasma Analysis

The gas distributions in the inner and outer region have been determined, but not the distributions for the partially ionized plasma. The gas is assumed to be completely coupled to the plasma in the plasma region. The plasma is partially ionized so that only 1-3% of the particles in this region are charged, the remainder being a high temperature neutral gas. Lehnert and Okada et al. have shown that this degree of ionization is sufficient to place the neutral gas in rotation [6, 13]. It is assumed that the neutral gas will have the same velocity distribution as the plasma. The rotational velocity of the plasma is determined by the magnitude of the crossed electric and magnetic fields

$$\vec{\omega} = \frac{\vec{E} \times \vec{B}}{rB^2} \quad (4.18)$$

where

$\vec{\omega}$ = angular velocity vector

\vec{E} = electric field

\vec{B} = magnetic field

B = magnitude of the magnetic field

r = radius of rotation.

Since the plasma and neutral gas are assumed to be coupled in the plasma region, the gas rotates with the same angular velocity as the plasma.

The low temperature, low density, partially ionized plasma used in this application may take on a number of velocity distributions. Lehnert shows that for low density plasmas, the plasma will have a

constant angular velocity. At higher densities the rotational velocity times the radius is shown to be constant [8]. A third distribution, constant rotational velocity, is also examined. The plasma density determines which of the following velocity distributions describe the plasma:

- 1) Isorotational case, $n = v_{\theta}/r = n_c = \text{constant}$
- 2) Constant rotational velocity, $n \times r = v_{\theta} = v_c = \text{constant}$
- 3) Constant velocity times position, $n \times r^2 = v_{\theta} \times r = \text{constant}$.

The velocity distribution in the plasma can be used to determine the pressure and density expressions. For the isorotational case

$$n_p = \text{const} \quad (4.19)$$

$$v_{\theta p}(r) = \text{const} \times r \quad (4.20)$$

$$\ln\left(\frac{p(r)}{p_0}\right) = \frac{\text{const}^2_m}{kT} \left(\frac{r^2 - r_1^2}{2}\right) \quad (4.21)$$

$$\ln\left(\frac{n(r)}{n_0}\right) = \frac{\text{const}^2_m}{kT} \left(\frac{r^2 - r_1^2}{2}\right) \quad (4.22)$$

where r_1 = radius of the inner gas-plasma interface.

The same relations may be found for the constant rotational velocity case

$$v_{\theta p} = \text{const} \quad (4.23)$$

$$n_p(r) = \text{const}/r \quad (4.24)$$

$$\ln\left(\frac{p(r)}{p_0}\right) = \left(\frac{\text{const}^2_m}{kT}\right) \ln\left(\frac{r}{r_1}\right) \quad (4.25)$$

$$\ln\left(\frac{n(r)}{n_0}\right) = \left(\frac{\text{const}^2_m}{kT}\right) \ln\left(\frac{r}{r_1}\right) \quad (4.26)$$

For the third distribution

$$v_{\theta p}(r) = \text{const}/r \quad (4.27)$$

$$n_p(r) = \text{const}/r^2 \quad (4.28)$$

$$\ln\left(\frac{p(r)}{p_0}\right) = \left(\frac{\text{const}^2 m}{kT}\right) \frac{1}{2} \left(\frac{1}{r_1^2} - \frac{1}{r^2}\right) \quad (4.29)$$

$$\ln\left(\frac{n(r)}{n_0}\right) = \left(\frac{\text{const}^2 m}{kT}\right) \frac{1}{2} \left(\frac{1}{r_1^2} - \frac{1}{r^2}\right) \quad (4.30)$$

The expressions may be used to determine the number densities for each isotope as a function of mass. The enrichment at any point can then be easily determined

$$N = \frac{n_{235}}{n_{235} + n_{238}} \quad (4.31)$$

where

N = enrichment in the ^{235}U isotope

n_{235} = number density of the ^{235}U isotope

n_{238} = number density of the ^{238}U isotope.

The process factor can be easily calculated from the number densities

$$\alpha = \frac{(n_{235}/n_{238})}{(n_{0\ 235}/n_{0\ 238})} \quad (4.32)$$

where

α = simple process factor

$n_{0\ 235}$ = number density of the ^{235}U isotope at some reference point r_0

$n_{0\ 238}$ = number density of the ^{238}U isotope at some reference point r_0 .

The computer program listed in the appendix combines these expressions to yield the angular velocity, rotational velocity, pressure ratio, number density, process factor, and enrichment at any point in the configuration for the three plasma distributions. The program may be used to analyze variations in parameters such as temperature, gas density, plasma thickness, gas thickness, wall position, or plasma critical velocity.

CHAPTER 5. PLASMA CENTRIFUGE FEASIBILITY

The feasibility of the plasma centrifuge technique may be evaluated theoretically by considering, among other things, the process factor, flow rate, and energy consumption. The process factor and flow rate may be used to evaluate the separative power of the element. The energy consumption can then be divided by the separative power to determine the energy that must be supplied per unit of product. In the construction of a demonstration device, a number of problems may be encountered. Some of the engineering problems that may be encountered will be discussed in Chapter 6.

The economic feasibility of a separation method must be determined by a number of related factors, including capital cost, process rate, and operating cost. For example, a high enrichment system requiring only a small number of stages may be economically competitive even if the capital cost per stage is high and the power consumption intense. Conversely, another technique may produce slightly enriched uranium at a lower cost even though the process factor is significantly lower. The second technique will require more stages than the first, but the capital cost per stage and energy requirement may be low enough to offset the disadvantage of the low process factor.

The plasma centrifuge will be similar to the first type of device described above; a device requiring a high capital cost and high energy consumption, with a high process factor. The energy consumption per unit of product may be reduced by maintaining a high flow rate. The process factor and mass flow rate are competing functions since the

high process rate is achieved by depleting the ^{238}U fraction at the inner wall, which reduces the flow rate. To consume the minimum amount of energy per unit of product, the system must produce both a large process factor and large mass flow rate.

In optimizing the system, several parameters must be considered. For example, the separation may be increased by decreasing the temperature of the system, increasing the angular velocity, or enlarging the physical dimensions of the device. With each of these options, increasing the process factor increases the pressure ratio across the device. Should the pressure ratio become too large, the gas density at the inner wall will become so low that no appreciable amount of enriched uranium can be extracted at this point. In this instance, although the process factor has been increased, the transverse mass flow rate has been decreased. Since the pressure ratio is a function of the mass of the isotope, and the process factor a function of the mass difference, the separative power will decrease with increasing process factors for characteristic plasma velocity and temperature parameters. The variation is discussed in detail in the section on the mass flow rate. The plasma centrifuge can not be optimized by variation of a single parameter such as flow rate, but rather by optimization of the mass flow and power consumption.

To evaluate the feasibility of the plasma centrifuge, the device must be analyzed with respect to a number of variables. A computer program was developed (Appendix A) to permit modeling of variations in the plasma and gas dimensions, as well as variations in temperature, density, velocity profile, feed fraction, and angular velocity. The

program lists variations in velocity, pressure, density, enrichment, and process factor for various locations across the configuration. The results of these models can be used to evaluate the feasibility of the plasma centrifuge. The results of these studies will aid in the design of a demonstration device to experimentally evaluate the technique.

Process Factor

The feasibility of the plasma centrifuge may be shown by consideration of the process factor, flow rate, and energy consumption. The process factor is dependent on a number of terms, including the plasma velocity distribution, the centrifuge configuration, the plasma temperature, and the critical velocity. Each of these parameters may alter the process factor, and affect the feasibility of the device. The variations in turn affect the mass flow rate and separative power, as discussed in the following section.

Plasma velocity distribution

The neutral gas will be coupled to the rotating plasma in the plasma region. The neutral gas velocity distribution will conform to the plasma velocity distribution. Equations 4.9, 4.16, and 4.21 show that the pressure ratio, and ultimately the process factor, are strongly dependent on the angular velocity. The velocity distribution of the plasma will control the process factor of the neutral gas.

In Chapter 4, the three plasma velocity distributions that were considered in this analysis were listed:

$$1) \quad \omega = \text{const} \quad (5.1)$$

$$2) \quad \omega \times r = \text{const} \quad (5.2)$$

$$3) \quad \omega \times r^2 = \text{const} \quad (5.3)$$

where

ω = angular velocity

r = radius at the point of interest.

The rotational velocity is related to the angular velocity by $v_{\theta} = \omega \times r$.

The three velocity distributions are dependent on the plasma density. Near the inner wall, where the plasma density is low, the first distribution ($\omega = \text{const}$) will determine the velocity [8]. At higher densities, the angular velocity will obey the third relation ($\omega \times r^2 = \text{const}$) [8]. The limiting densities and transition points are not currently defined. The discussion in Chapter 4 lists the determination of the plasma density and velocity distribution as a field of active research. A third distribution ($\omega \times r = \text{const}$) is also considered. Although the exact distribution must be known to design the device, it will be shown that modification of the configuration and variation of plasma parameters can produce adequate separation for any of the distributions considered.

To evaluate the distribution across the configuration, the constant in Equations 5.1, 5.2, and 5.3 must be determined. Due to instabilities at the end insulators, the rotational velocity of the plasma will be limited to a specific value at that point [4], as given by

$$v_c = (2e\phi_i/m_i)^{1/2} \quad (5.4)$$

where

v_c = critical rotational velocity

e = charge of the ion

ϕ_i = ionization potential

m_i = mass of the ion.

An ionization potential of 6 V will produce a critical velocity of about 2200 m/sec. This value is characteristic of values used in other analyses and in operating devices [8, 13]. Figure 2.3 and Fig. 4.1 show that the end insulators are located at or inside a radius of 0.1 m for typical centrifuge designs. Assuming that the device attains the critical velocity at a radius of 0.1 m, each of the constants in Equations 5.1, 5.2, and 5.3 may be evaluated. Figure 2.3 and Fig. 4.1 also show the plasma as being about 5 cm in width and extending from about 5 cm to 30 cm. As a standard for analysis, a configuration will be analyzed with boundary walls at 5 and 20 cm and a plasma width of 5 cm, extending from 10 to 15 cm. Figure 4.2 is an example of such a configuration. The axial length of the experimental device is currently about 0.8 m. Although these values are characteristic of current rotating plasmas, design optimization of the plasma centrifuge may produce considerable modification. The dimensions do provide a basis of comparison.

The centrifuge configuration with walls at 5 and 20 cm and plasma edges at 10 and 15 cm permits easy comparison of the 3 velocity profiles. The rotational velocity in the inner and outer gas regions is determined by the rotational velocity at the plasma edge, which is a boundary condition in the Navier-Stokes equation. Figure 5.1 is an

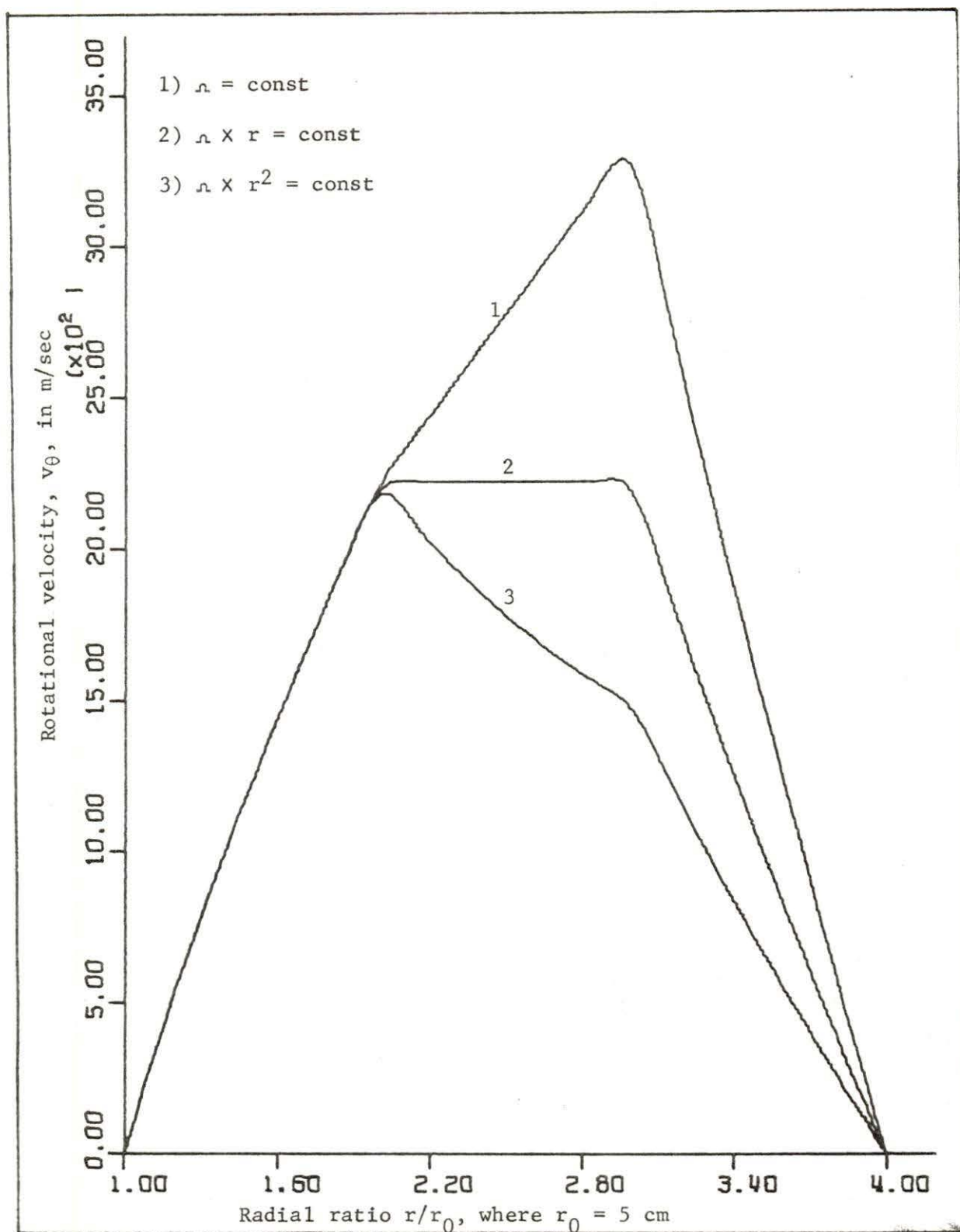


Fig. 5.1. Velocity distribution.

example of such a distribution. Since the plasma attains the same critical velocity of 2200 m/s at a radius of 0.1 m, the velocity distribution for the inner gas region is the same for each case. The three velocity distributions produce different profiles for the plasma region, and different boundary conditions for the outer gas region.

The difference in the velocity distributions produces large differences in the process factor. Figure 5.2 shows the variation in the process factor across the configuration for the three velocity distributions. Since the velocity profile is the same for the inner gas for each distribution, the process factor is the same. Higher velocities produce higher process factors. The first distribution produces the highest velocity profile with a process factor of 1.21, while the lowest distribution produces a process factor of only 1.10.

Configuration

The process factor is also a function of the plasma centrifuge configuration. Since the plasma angular velocity is position dependent, the process factor will be spatially dependent. In addition, the process factor will be a function of the width of the gas region. Larger region widths produce larger centrifugal forces which increase the separation and process factor. Tables 5.1, 5.2, and 5.3 show the spatial dependence of the process factor for each of the plasma velocity distributions. In each case, larger region widths increase the process factor. Configurations producing the largest angular velocity produce the highest process factor, as indicated by Fig. 5.2.

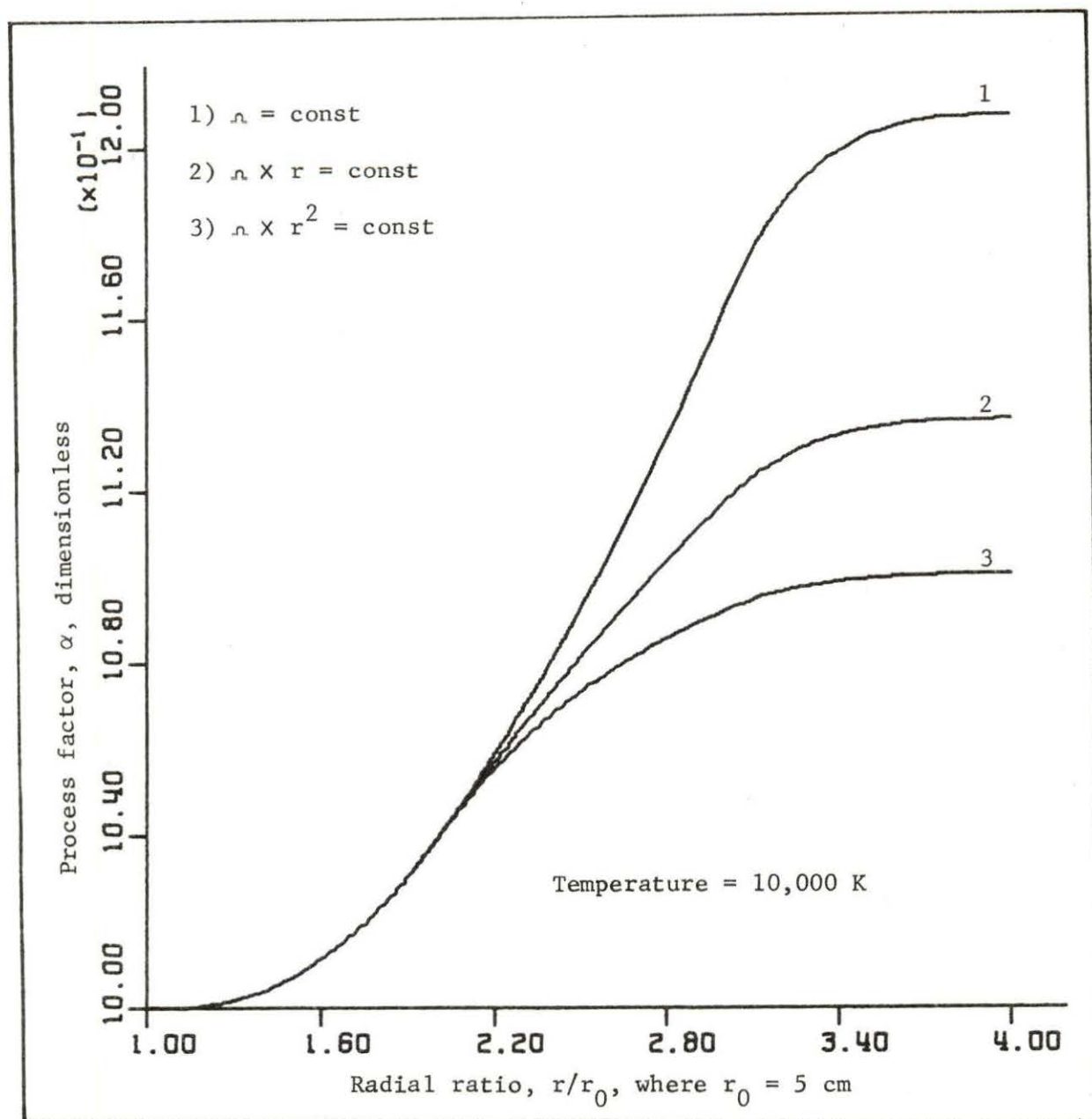


Fig. 5.2. Process factor as a function of velocity distribution.

Table 5.1. Spatial distribution, $\omega = \text{constant}$ ^a

Configuration, cm				Process factor ^b , by region			Pressure ratio, by region		
R1	R2	R3	R4	Inner	Plasma	Outer	Inner	Plasma	Outer
5	10	15	20	1.039	1.118	1.039	2.15×10^1	6.80×10^3	2.04×10^1
7	10	15	20	1.021	1.118	1.039	5.21×10^0	6.80×10^3	2.04×10^1
8	13	15	20	1.048	1.051	1.039	4.23×10^1	5.21×10^1	2.04×10^1
9	14	15	20	1.051	1.026	1.039	5.31×10^1	7.74×10^0	2.04×10^1
10	15	20	22	1.054	1.168	1.023	6.68×10^1	1.33×10^5	6.02×10^0
10	14	17	20	1.039	1.087	1.028	2.13×10^1	7.10×10^2	9.06×10^0
12	15	20	22	1.030	1.168	1.023	1.05×10^1	2.32×10^5	6.02×10^0
15	17	20	25	1.022	1.103	1.054	5.47×10^0	2.53×10^3	6.49×10^1
15	20	22	25	1.070	1.078	1.037	2.12×10^2	3.76×10^2	1.83×10^1
17	20	22	25	1.039	1.078	1.037	2.11×10^1	3.76×10^2	1.83×10^1
18	22	25	27	1.059	1.134	1.029	9.44×10^1	2.10×10^4	9.61×10^0
20	22	25	27	1.028	1.133	1.029	8.76×10^0	2.10×10^4	9.60×10^0
20	25	27	30	1.086	1.096	1.047	6.79×10^2	1.54×10^3	3.71×10^1
22	25	27	30	1.048	1.097	1.047	4.27×10^1	1.54×10^3	3.71×10^1
23	25	27	30	1.031	1.097	1.047	1.16×10^1	1.54×10^3	3.70×10^1

^aR1 = radius of inner wall, R2 = radius of inner plasma edge, R3 = radius of outer plasma edge, R4 = radius of outer wall.

^bTemperature = 10,000 K, $v_c = 2000$ m/sec.

Table 5.2. Spatial distribution, $\omega \times \text{radius} = \text{constant}$ ^a

Configuration, cm ^a				Process factor ^b , by region			Pressure ratio, by region		
R1	R2	R3	R4	Inner	Plasma	Outer	Inner	Plasma	Outer
5	10	15	20	1.039	1.075	1.017	21.47	306.	3.82
7	10	15	20	1.021	1.075	1.017	5.21	306.	3.82
8	13	15	20	1.028	1.026	1.017	9.16	7.54	3.82
9	14	15	20	1.026	1.012	1.017	7.59	2.65	3.82
10	15	20	22	1.024	1.052	1.006	6.47	58.1	1.57
10	14	17	20	1.020	1.035	1.010	4.76	15.51	2.14
12	15	20	22	1.013	1.052	1.006	2.84	58.07	1.57
15	17	20	25	1.007	1.029	1.013	1.80	4.92	2.84
15	20	22	25	1.017	1.017	1.008	3.82	3.84	1.82
17	20	22	25	1.010	1.017	1.008	2.14	3.84	1.82
18	22	25	27	1.012	1.023	1.004	2.56	6.08	1.44
20	22	25	27	1.006	1.023	1.004	1.57	6.08	1.44
20	25	27	30	1.013	1.014	1.006	2.84	2.96	1.64
22	25	27	30	1.008	1.014	1.006	1.82	2.96	1.64
23	25	27	30	1.005	1.014	1.006	1.48	2.96	1.64

^aR1 = radius of inner wall, R2 = radius of inner plasma edge, R3 = radius of outer plasma edge, R4 = radius of outer wall.

^bTemperature = 10,000 K, $v_c = 2200$ m/sec.

Table 5.3. Spatial distribution, $\omega \times (\text{radius})^2 = \text{constant}^a$

Configuration, cm ^a				Process Factor ^b , by region			Pressure ratio, by region		
R1	R2	R3	R4	Inner	Plasma	Outer	Inner	Plasma	Outer
5	10	15	20	1.039	1.051	1.010	21.47	50.50	1.81
7	10	15	20	1.021	1.051	1.007	5.21	50.50	1.81
8	13	15	20	1.017	1.013	1.008	3.71	2.83	1.81
9	14	15	20	1.013	1.006	1.007	2.81	1.59	1.81
10	15	20	22	1.010	1.013	1.001	2.29	3.95	1.12
10	14	17	20	1.010	1.015	1.003	2.22	3.19	1.30
12	15	20	22	1.006	1.017	1.001	1.59	3.95	1.12
15	17	20	25	1.002	1.009	1.003	1.23	1.97	1.30
15	20	22	25	1.004	1.004	1.002	1.40	1.36	1.13
17	20	22	25	1.002	1.004	1.002	1.21	1.36	1.13
18	22	25	27	1.002	1.004	1.001	1.21	1.39	1.06
20	22	25	27	1.001	1.004	1.001	1.10	1.39	1.06
20	25	27	30	1.002	1.002	1.001	1.18	1.18	1.07
22	25	27	30	1.001	1.002	1.001	1.10	1.18	1.07

^aR1 = radius of inner wall, R2 = radius of inner plasma edge, R3 = radius of outer plasma edge, R4 = radius of outer wall.

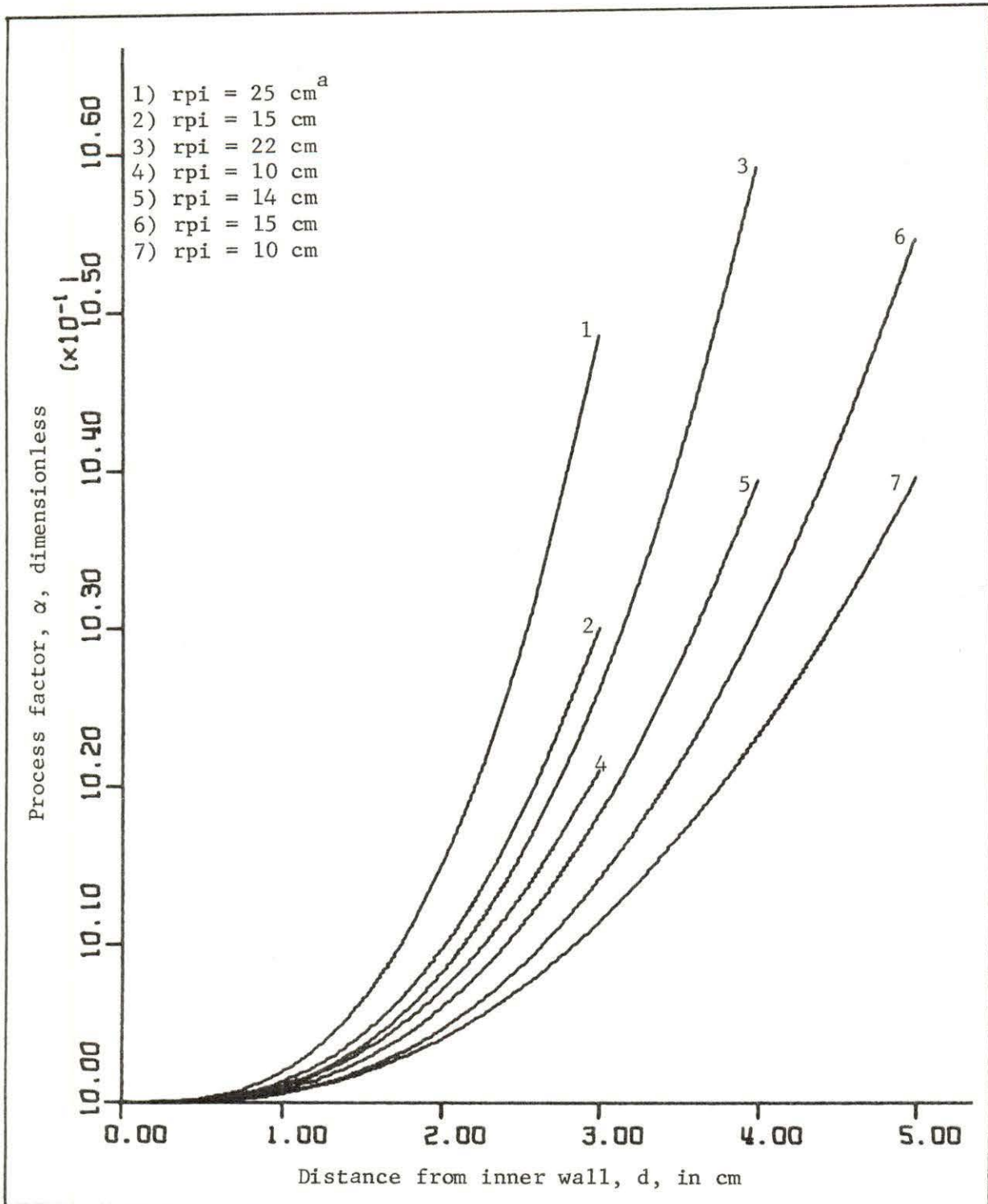
^bTemperature = 10,000 K, $v_c = 2200$ m/sec.

Figures 5.3, 5.4, and 5.5 show the distribution in graphical form. The figures show the process factor for the inner gas region as a function of position. The position is the distance from the inner boundary wall. Larger region widths and larger angular velocities produce the largest process factors. The curve with an inner plasma radius of 10 cm is the same for each of the three figures, since this is the same curve for the three distributions shown in Fig. 5.2. The curve provides a basis for comparison between the distributions. The figures show that large process factors can be obtained by adjusting the location of the plasma and the width of the gas regions.

Plasma parameters

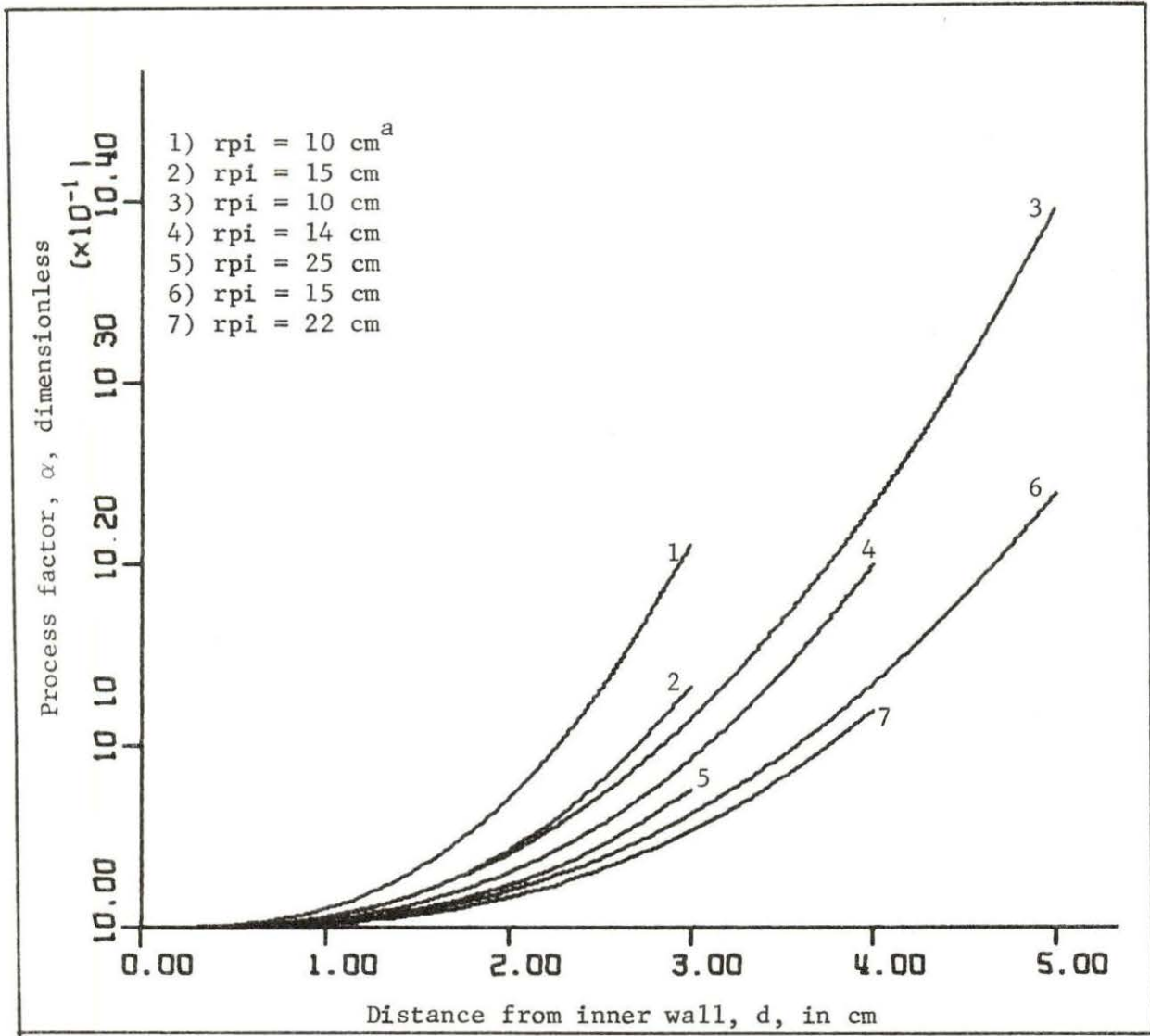
The process factor may also be controlled by adjustment of the plasma parameters. The process factor may be increased by increasing the critical velocity of the plasma or by decreasing the operating temperature. Since the process factor may be controlled by the centrifuge configuration, only the first plasma velocity distribution ($\omega = \text{const}$) will be considered in this analysis. Similar values may be obtained for the additional distributions (Appendix B).

Table 5.4 shows the variation in the process factor as a function of angular velocity. The values are listed by region. The process factor across the configuration will be the product of the process factor for the three regions. Figure 5.6 shows the same distribution in graphical form. Large values for the critical angular velocity produce large process factors.



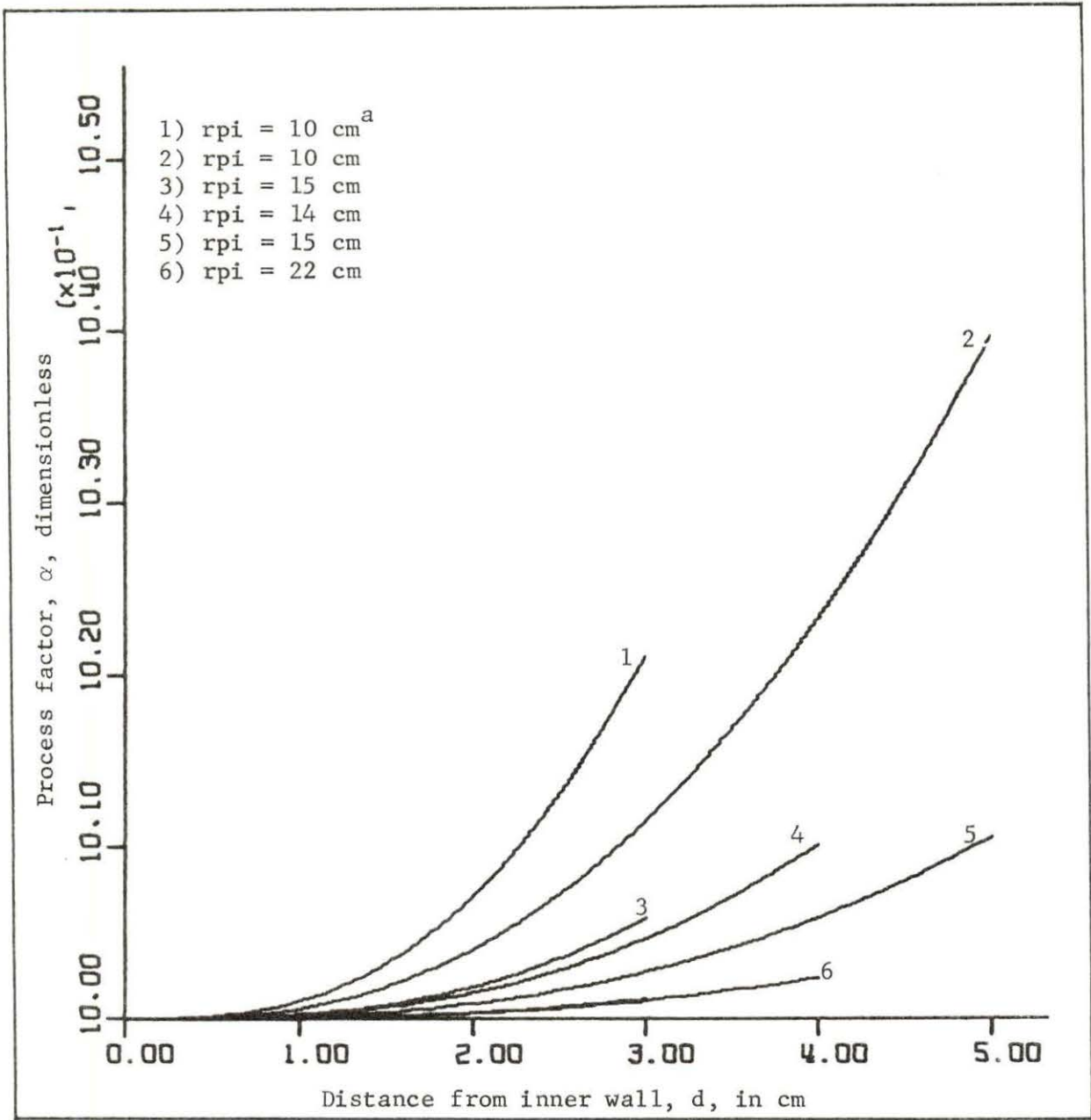
^a r_{pi} = radius of the inner plasma edge, temperature = 10,000 K.

Fig. 5.3. Process factor versus distance, where $n = \text{const.}$



^a r_{pi} = radius of inner plasma edge, temperature = 10,000 K.

Fig. 5.4. Process factor versus distance, where $n \times r = \text{const.}$



^a r_{pi} = radius of the inner plasma edge, temperature = 10,000 K.

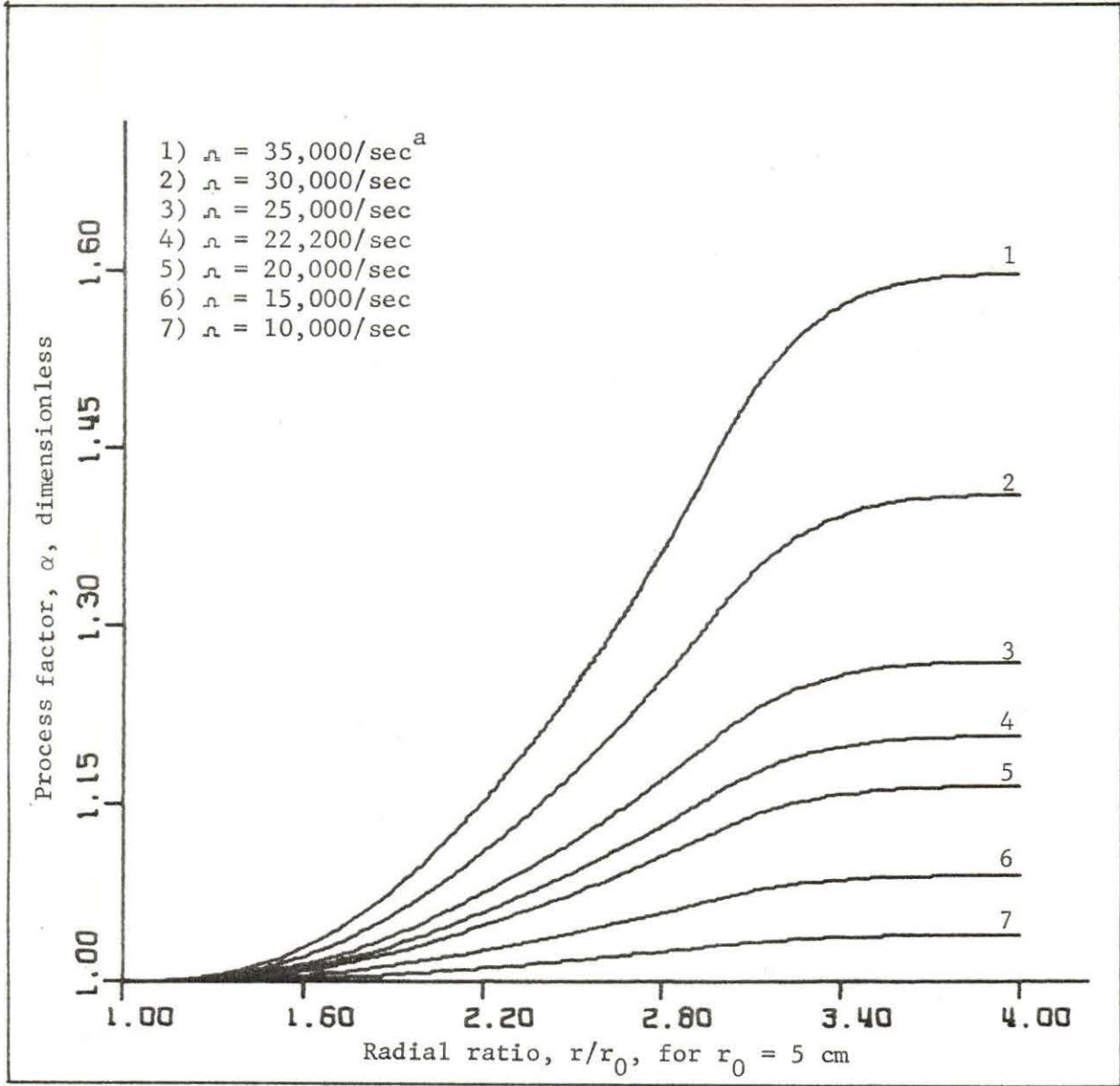
Fig. 5.5. Process factor versus distance, where $n \times r^2 = \text{const.}$

Table 5.4. Angular velocity distribution, $\omega = \text{constant}$ ^a

Angular velocity in sec^{-1}	Process factor, by region			Pressure ratio, by region		
	Inner	Plasma	Outer	Inner	Plasma	Outer
40,000	1.134	1.435	1.131	2.11×10^4	2.76×10^{12}	1.77×10^4
35,000	1.101	1.318	1.099	2.04×10^3	3.35×10^9	1.79×10^3
30,000	1.073	1.225	1.072	2.70×10^2	9.96×10^6	2.45×10^2
25,000	1.050	1.151	1.049	4.89×10^1	7.24×10^4	4.57×10^1
23,000	1.042	1.127	1.042	2.99×10^1	1.30×10^4	2.57×10^1
22,000 ^b	1.039	1.118	1.039	2.15×10^1	6.80×10^3	2.04×10^1
21,000	1.035	1.105	1.034	1.56×10^1	2.69×10^3	1.48×10^1
20,000	1.032	1.094	1.031	1.20×10^1	1.29×10^3	1.15×10^1
18,000	1.026	1.076	1.025	7.50×10^0	3.31×10^2	7.20×10^0
15,000	1.018	1.052	1.018	4.06×10^0	5.62×10^1	3.96×10^0
12,000	1.011	1.034	1.010	2.45×10^0	1.32×10^1	2.41×10^0
10,000	1.008	1.023	1.008	1.86×10^0	5.99×10^0	1.84×10^0

^a Assuming boundary walls at 5 and 20 cm, plasma edges at 10 and 15 cm, and temperature = 10,000 K.

^b Critical angular velocity at a radius of 0.1 m.



^a ω = angular velocity, temperature = 10,000 K.

Fig. 5.6. Process factor as a function of angular velocity, where $\omega = \text{const.}$

Similar results are found for the temperature distribution. Lower temperatures increase the process factor. Table 5.5 shows the variation in the process factor as a function of temperature for the same centrifuge configuration. Process factors in excess of 3 are predicted for this configuration at an operating temperature of 1500 K.

Process factor

An important conclusion may now be drawn concerning the feasibility of the plasma centrifuge: High process factors may be attained regardless of the plasma velocity distribution or plasma location. By adjusting the critical velocity, temperature, and gas width, extremely large process factors may be predicted.

Process factors of 3 are not physically attainable. The system is capable of producing such separation, but not of using the separation. Tables 5.4 and 5.5 also show the pressure ratio as a function of angular velocity and temperature, respectively. Very large process factors can only be produced by depleting the ^{238}U number density at the inner wall. Since there is only a small mass difference between ^{235}U and ^{238}U , the ^{235}U number density will also be reduced. The enriched fraction must be extracted from the low density gas at the inner wall, which results in a decreased mass flow rate.

Figure 5.7 shows the pressure ratio across the configuration as a function of angular velocity. High velocity values produce pressure ratios, in some cases, in excess of 10^{15} . Only a finite amount of gas is confined in the device. As the pressure ratio increases, the gas becomes depleted at the inner wall, while the gas pressure at the

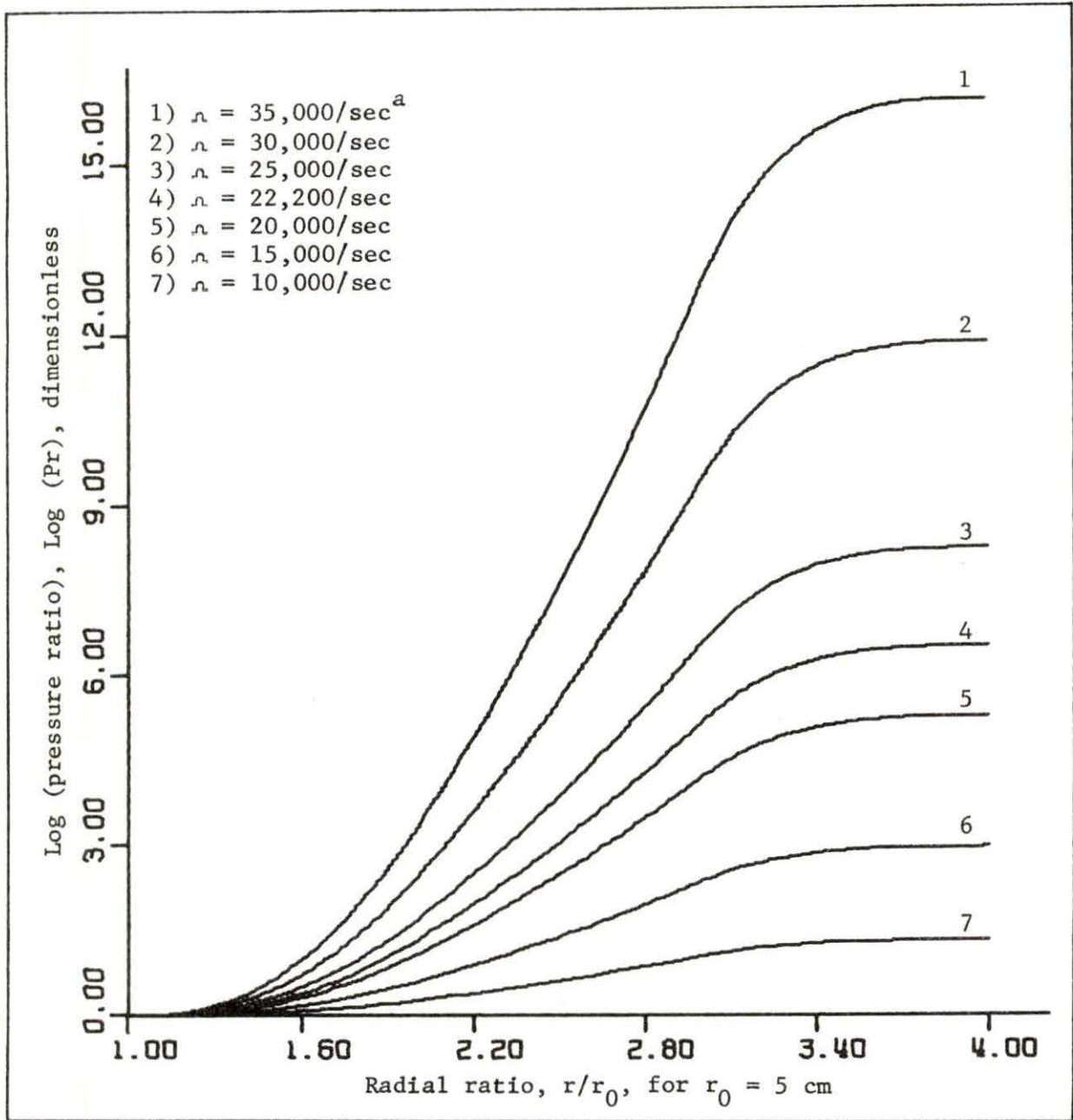
Table 5.5. Temperature distribution, $\omega = \text{constant}^a$

Temperature	Process factor, by region			Pressure ratio, by region		
	Inner	Plasma	Outer	Inner	Plasma	Outer
15,000	1.026	1.077	1.026	7.72×10^0	3.59×10^2	7.46×10^0
10,000 ^b	1.039	1.123	1.039	2.15×10^1	6.80×10^3	2.04×10^1
9,000	1.044	1.132	1.043	3.02×10^1	1.81×10^4	2.84×10^1
8,000	1.050	1.149	1.049	4.62×10^1	6.17×10^4	4.32×10^1
7,000	1.057	1.172	1.056	7.99×10^1	2.98×10^5	7.40×10^1
6,000	1.066	1.204	1.065	1.66×10^2	2.44×10^6	1.52×10^2
5,000	1.080	1.249	1.079	4.61×10^2	4.62×10^7	4.14×10^2
4,000	1.101	1.320	1.100	2.14×10^3	3.81×10^9	1.87×10^3
3,000	1.138	1.449	1.135	2.75×10^4	5.95×10^{12}	2.30×10^4
2,500 ^c	1.167	1.560	1.164	2.12×10^5	2.13×10^{15}	1.72×10^5
2,000	1.213	1.744	1.209	4.56×10^6	1.45×10^{19}	3.49×10^6
1,500	1.294	2.099	1.288	7.56×10^8	3.54×10^{25}	5.30×10^8

^aAssuming boundary walls at 5 and 20 cm, and plasma edges at 10 and 15 cm, $v_c = 2200$ m/sec.

^bTemperature assumed in the analysis by Lehnert [8].

^cTemperature assumed in the analysis by Okada et al. [13].



^a $\omega =$ angular velocity, temperature = 10,000 K.

Fig. 5.7. Pressure ratio as a function of angular velocity, where $\omega =$ const.

outer wall only increases moderately. Table 5.6 shows this relationship for all three distributions. While the density decreases by 15 orders of magnitude at the inner wall, the density at the outer wall does not even double. Table 5.7 shows similar results for the temperature distribution.

The plasma centrifuge could produce large separation factors. The system becomes limited though due to extraction of the low density gas at the inner wall. The feasibility of the centrifuge must be evaluated by considering both the process factor and flow rate. The following section derives the expression for the separative power, and evaluates realistic values for both the process factor and mass flow rate.

Mass Flow Rate

The plasma centrifuge can produce a separation factor sufficiently high to produce slightly enriched uranium at the inner wall. In addition, the device must produce a sufficient quantity of product, at a cost competitive with alternative enrichment schemes.

The mass flow rate may be evaluated by determining the separative power of the device. An isotope separation element will produce two product streams, an enriched fraction and a depleted fraction. A mass balance may be performed on the stage,

$$N = \theta N' + (1 - \theta)N'' \quad (5.5)$$

where

N = mole fraction of the feed material

Table 5.6. Velocity produced wall limitations^a

Plasma distribution	Angular velocity in sec ⁻¹	Density, M ^{-3b}		Enrichment ^c	
		Inner wall	Outer wall	Inner wall	Outer wall
n = const	40,000	7.30 × 10 ³	7.49 × 10 ²⁴	1.295%	0.7084%
	25,000	3.56 × 10 ¹⁶	5.74 × 10 ²⁴	0.897%	0.7085%
	15,000	4.78 × 10 ²¹	4.31 × 10 ²⁴	0.771%	0.7083%
n × r = const	40,000	3.11 × 10 ¹⁰	5.95 × 10 ²⁴	1.070%	0.7085%
	25,000	1.21 × 10 ¹⁹	4.60 × 10 ²⁴	0.832%	0.7085%
	15,000	3.36 × 10 ²²	3.42 × 10 ²⁴	0.750%	0.7082%
n × r ² = const	40,000	9.72 × 10 ¹⁹	4.78 × 10 ²⁴	0.964%	0.7086%
	25,000	2.47 × 10 ²⁰	3.71 × 10 ²⁴	0.799%	0.7086%
	15,000	8.85 × 10 ²²	2.82 × 10 ²⁴	0.740%	0.7086%

^a Assuming boundary walls at 5 and 20 cm, plasma edges at 10 and 15 cm.

^b Assuming an initial gas density of 10²² M⁻³, temperature = 10,000 K.

^c Assuming a feed enrichment of 0.711% ²³⁵U.

Table 5.7. Temperature produced wall limitations^a

Plasma distribution	Temperature, K	Density, M ⁻³ ^b		Enrichment ^c	
		Inner wall	Outer wall	Inner wall	Outer wall
n = const	10,000	1.81 × 10 ¹⁸	5.38 × 10 ²⁴	0.854%	0.7085%
	7,000	3.37 × 10 ¹⁵	5.93 × 10 ²⁴	0.925%	0.7085%
	3,000	2.02 × 10 ³	7.55 × 10 ²⁴	1.317%	0.7084%
n × r = const	10,000	1.72 × 10 ²⁰	4.31 × 10 ²⁴	0.804%	0.7085%
	7,000	2.47 × 10 ¹⁸	4.75 × 10 ²⁴	0.849%	0.7086%
	3,000	1.30 × 10 ¹⁰	6.00 × 10 ²⁴	1.080%	0.7085%
n × r ² = const	10,000	1.77 × 10 ²¹	3.48 × 10 ²⁴	0.779%	0.7086%
	7,000	7.56 × 10 ¹⁹	3.83 × 10 ²⁴	0.811%	0.7086%
	3,000	5.07 × 10 ¹³	4.81 × 10 ²⁴	0.972%	0.7086%

^aAssuming boundary walls at 5 and 20 cm, plasma edges at 10 and 15 cm.

^bAssuming an initial gas density of 10²² M⁻³, temperature = 10,000 K.

^cAssuming a feed enrichment of 0.711% ²³⁵U.

N' = mole fraction of the product stream

N'' = mole fraction of the stripped stream

θ = flow fraction in the product stream (cut).

The mole fraction of the enriched and stripped streams is a function of the separation element and feed material. In general

$$R' = \alpha_e R \quad (5.6)$$

$$R'' = \left(\frac{1}{\alpha_s}\right)R \quad (5.7)$$

where

α_e = simple process factor for enrichment

α_s = simple process factor for stripping

R' = molecular abundance ratio of the enriched fraction

R'' = molecular abundance ratio of the stripped fraction

R = molecular abundance ratio of the feed.

The abundance ratio and mole fraction are related by the following expressions

$$R = \frac{N}{1 - N} \quad (5.8)$$

$$N = \frac{R}{1 + R} \quad (5.9)$$

Cohen [20] has shown that the separation elements will be used at their optimum efficiency when they are confined in an ideal cascade. An ideal cascade will minimize the number of separating elements in any section of a cascade. Furthermore, the optimum rate of production of a stage will occur when the concentration gradient is

half its value at the point of no production. Finally, the production rate will be at a maximum when the cut is close to 1/2 [20].

The constraints of the ideal cascade may then be imposed to evaluate the productivity of any enrichment scheme. A function U is derived to represent the value of a quantity of separated material

$$U = FV(N) \quad (5.10)$$

where

F = number of moles of material

$V(N)$ = value function.

The value function $V(N)$ should not be confused with the price of the material. The function produces a dimensionless quantity that can be used to fix a "value" per unit of material [20].

Equation 5.10 may be used to define a net change in value of the material passing through the enrichment element,

$$\delta U = \theta GV(N') + (1 - \theta)GV(N'') - GV(N) \quad (5.11)$$

where

G = material process rate, in moles per unit time

θ = cut

$V(N)$ = value of the feed material

$V(N')$ = value of the enriched fraction

$V(N'')$ = value of the stripped fraction.

An additional quantity, the process difference, may be defined by the process factor

$$\epsilon = \alpha - 1 \quad (5.12)$$

Assuming that ϵ is much less than unity, and that the value functions are expanded in a Taylor series about N , the following expression for δU is obtained

$$\begin{aligned} \delta U = V(N) [\theta G + (1 - \theta)G - G] + \frac{dV(N)}{dN} [\theta G(N' - N) + (1 - \theta)G(N'' - N)] \\ + \frac{d^2V(N)}{dN^2} \left[\theta G \frac{(N' - N)^2}{2} + (1 - \theta)G \frac{(N'' - N)^2}{2} \right] + \dots \end{aligned} \quad (5.13)$$

By the conservation of matter

$$\theta(N' - N) = - (1 - \theta)(N'' - N) \quad (5.14)$$

$$N' - N = N(1 - N) \quad (5.15)$$

The coefficients of $V(N)$ and $dV(N)/dN$ will vanish, leaving

$$\delta U = \frac{\theta}{1 - \theta} \frac{G\epsilon^2}{2} \frac{d^2V(N)}{dN^2} [N(1 - N)]^2 \quad (5.16)$$

In order that Equation 5.16 be independent of the mole fraction, the following expression must hold

$$\frac{d^2V(N)}{dN^2} = \frac{1}{[N(1 - N)]^2} \quad (5.17)$$

Equation 5.16 simplifies to the following,

$$\delta U = \frac{\theta}{1 - \theta} \frac{G\epsilon^2}{2} \quad (5.18)$$

The function δU may be used to evaluate different enrichment schemes since it is a measure of the net change in value of a single element. The term is known as the separative power of the enrichment element. The change in value is independent of the mole fraction of the material.

If a total value change of ΔU is desired, the number of elements required to produce this change may be calculated

$$S = \frac{\Delta U}{\delta U} \quad (5.19)$$

where

S = total number of elements

ΔU = change in value

δU = separative power per element.

The value function may also be solved by using Equation 5.17

$$\frac{d^2 V(N)}{dN^2} = \frac{1}{[N(1 - N)]^2} \quad (5.17)$$

The equation is solved to yield

$$V(N) = c_0 + c_1 N + (2N - 1) \ln\left(\frac{N}{1 - N}\right) \quad (5.20)$$

where c_0 and c_1 are constants of integration. The equimolar mixture may be assigned a value of 0

$$V(0.5) = \frac{dV(0.5)}{dN} = 0 \quad (5.21)$$

The value function then reduces to the following

$$V(N) = (2N - 1) \ln\left(\frac{N}{1 - N}\right) \quad (5.22)$$

The value function may be used to evaluate the separative work that the element can produce. The separative power is a measure of the value of the element, regardless of mole fraction. The separative work provides a measure of the work required to obtain a desired

mole fraction. The separative work may be evaluated from the following equation [21]

$$\frac{\Delta}{L} = \frac{N' - N}{N - N''} V(N'') + V(N') - \frac{N' - N''}{N - N''} V(N) \quad (5.23)$$

where

Δ = separative work

L = unit of product material

N' = mole fraction of product

N = mole fraction of feed

N'' = mole fraction of waste

$V(N)$ = the value function defined by Equation 5.22.

Equation 5.23 may be used to assign a value to the separative work needed to produce uranium of a desired enrichment. Traditionally, the assay weight fraction of the tailstream has been 0.2% ^{235}U . Natural uranium feed contains 0.711% ^{235}U . These values may be used in Equation 5.17 to produce the table shown in Fig. 5.8 [21]. The table shows that the production of 2% ^{235}U would require 2.194 kg SWU/kg product. The product of Equation 5.18 and Equation 5.23 may be used to evaluate the separative power per element in units of kg SWU per unit time.

The plasma centrifuge may be compared with other enrichment methods by comparing the separative power of an individual element. To calculate this term, values must be determined for the cut (θ), the enrichment process difference (ϵ), the mass flow rate (G), and the mole fraction of the product (N'). For the ideal cascade, the cut should be equal to 1/2. The process difference, mass flow rate, and mole fraction are

Standard table of enriching services*		
Assay, wt.% ^{235}U	Feed component (normal), kg U feed/kg U product	Separative work component, kg SWU/kg product
0.20	0	0
0.30	0.196	-0.158
0.40	0.391	-0.198
0.50	0.587	-0.173
0.60	0.783	-0.107
0.70	0.978	-0.012
0.711 (normal)	1.000	0.000
0.80	1.174	0.104
0.90	1.370	0.236
1.00	1.566	0.380
1.20	1.957	0.698
1.40	2.348	1.045
1.60	2.740	1.413
1.80	3.131	1.797
2.00	3.523	2.194
2.20	3.914	2.602
2.40	4.305	3.018
2.60	4.697	3.441
2.80	5.088	3.871
3.00	5.479	4.306
3.40	6.262	5.191
3.80	7.045	6.090
4.00	7.436	6.544
5.00	9.393	8.851
10.00	19.178	20.863
90.00	175.734	227.341
98.00	191.389	269.982

*The kilograms of feed and separative-work components for assays not shown can be determined by linear interpolation between the nearest assays listed.

Fig. 5.8. Table of enriching services [21].

all functions of the device configuration. Each of these parameters, in addition to several others, are dependent upon one another. For example, the pressure ratio is dependent on the initial gas density. The initial gas density is restricted by the magnitude of the axial magnetic field, which is in turn dependent on the degree of ionization and plasma density, with the plasma density dependent on temperature and gas density, etc.

To evaluate the above parameters, realistic constraints may be imposed on the system. The constraints define bounds for the analysis and permit comparison with previous work on the plasma centrifuge. In the last section it was shown that separation could be produced at any location or velocity distribution. As an example, consider the effect of temperature variations on gas parameters. Table 5.5 shows that the process factor increases as the temperature decreases, as does the pressure ratio. The important point is that although the gas density becomes very low near the inner wall, only moderate increases occur at the outer wall. Similar results are observed for variations in the angular velocity and region width.

The gas density at the outer wall must be prevented from becoming so large that heavy reinforcement material is required, causing inhomogeneities in the magnetic field and prohibitively high construction costs. An initial gas density of 10^{22} part/m³ produces outer wall densities on the order of 10^{24} part/m³, regardless of inner wall densities. A gas number density of 5×10^{24} part/m³ at 10,000 K produces a pressure of about 100 psi. This pressure is easily met by containment structures, and the initial density provides sufficient ionization

without producing a plasma density that would require a large magnetic field to confine the plasma.

The gas pressure at the inner wall should be maintained as high as possible to produce high flow rates, while still producing a high separation factor. The density and enrichment are competing functions in a centrifuge. Lehnert [8] has performed an analysis using a pressure ratio of 100 with a process factor of about 1.06. A similar analysis by Okada et al. [13] used a pressure ratio of 10^7 with a process factor of 1.25. Similar analyses can produce pressure ratios of even 10^{15} with process factors approaching 2.0. An optimization study is needed to determine the device configuration that produces the maximum separation per element. A pressure ratio of about 10^5 produces inner wall densities on the order of 10^{19} , providing both high flow rates and high enrichment.

The determination of the outer wall density and pressure ratio determines the inner wall gas density, process difference, and mole fraction. The mass flow rate must still be evaluated. The mass flow rate suffers a number of constraints:

- 1) The cut must equal $1/2$ for the ideal cascade
- 2) The Mach number for axial flow at the inner wall must be less than unity
- 3) The system must complete the separation in the device dimensions
- 4) The size and orientation of the extraction probe must not create mixing or decrease separation.

The Mach number is the ratio of the gas velocity to the speed of sound in the medium

$$M = \frac{v_z}{a} \quad (5.24)$$

where

M = Mach number

v_z = velocity in the axial direction

a = speed of sound.

The speed of sound is given by the following expression

$$a = (\gamma RT)^{1/2} \quad (5.25)$$

where

γ = ratio of specific heats, $\gamma = c_p/c_v$

R = universal gas constant = 8.3143 J/mol K

T = temperature.

For a high temperature uranium gas, $\gamma = 1.433$. The axial velocity at the inner wall can then be determined from the Mach number. This velocity and gas density can be used to evaluate the flow rate at the inner wall. Since the cut will be 1/2 for the ideal cascade, the total flow should be twice the flow that is extracted at the inner wall.

$$\text{Total flow} = \frac{v_z \bar{n}_i A_i}{\theta} \quad (5.26)$$

where

\bar{n}_i = average gas density over the extraction area

A_i = extraction area

θ = cut.

The total flow must also be given by the continuity equation

$$\bar{n}A\bar{v} = \text{constant} \quad (5.27)$$

where

\bar{n} = average gas number density across the configuration

A = total flow area

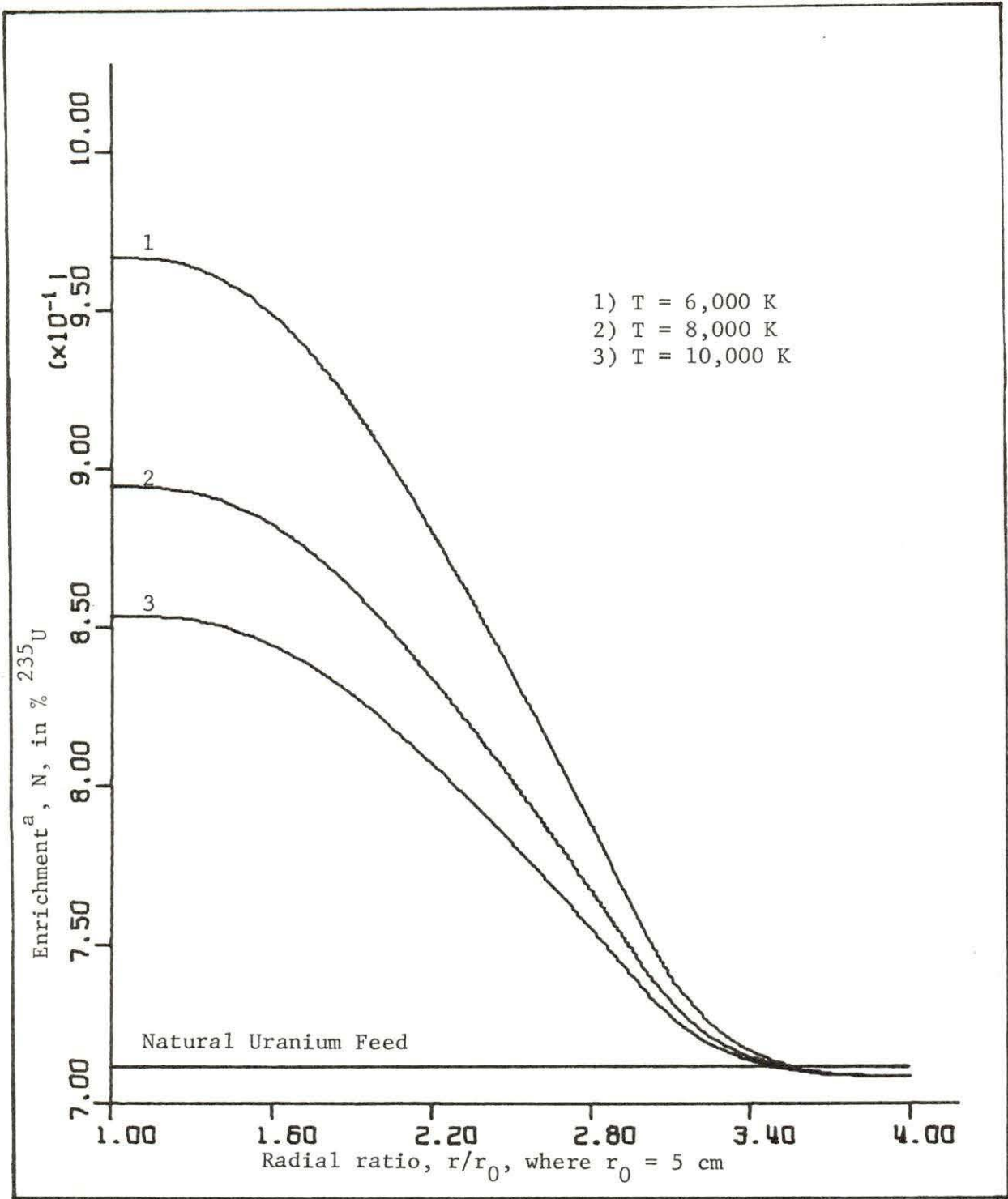
\bar{v} = average axial velocity of the gas.

The flow at any point in the configuration may be evaluated from the continuity equation

$$\begin{aligned} \bar{n}A\bar{v} &= \sum_{i=1}^N n_i A_i v_i \\ &= n_1 v_1 A_1 + n_2 v_2 A_2 + n_3 v_3 A_3 + \dots \end{aligned} \quad (5.28)$$

The equation is valid if $\bar{nv} = \bar{n}_i \bar{v}_i$.

The plasma centrifuge poses some characteristic problems with respect to an ideal cascade. Figure 5.9 shows that although high enrichment is achieved at the inner edge, only a small depletion will occur at the outer wall. The result is that if the enriched and stripped streams maintain the same flow rate ($\theta = 1/2$), the gas in the device will become depleted in the light fraction. To maintain the same molar concentration in the device, the stripped fraction must have a much larger flow than the enriched stream. The differences in flow rates produce a smaller cut, resulting in a lower separative power. The small depletion at the outer wall will pose serious problems in the cascade construction, since a large number of stages will be required to deplete the gas. Before considering the construction of a cascade,



^a Assuming constant angular velocity

Fig. 5.9. Enrichment as a function of temperature.

consider the feasibility of a discrete element. The cascade limitations will be discussed at the end of this section.

Consider the separative power of a partially ionized plasma centrifuge. Assume that the following conditions hold for the configuration and plasma parameters:

- 1) Boundary walls are located at 5 and 20 cm
- 2) Plasma region extends from 10 to 15 cm
- 3) Plasma angular velocity is constant at $20,000 \text{ sec}^{-1}$
- 4) Plasma and gas temperature are constant in space at 10,000 K
- 5) Initial gas density is 10^{22} part/m^3
- 6) Feed gas is natural uranium, with a molar concentration of $0.00711 \text{ }^{235}\text{U}$.

A plasma centrifuge under such conditions would produce an outer wall density of $5.08 \times 10^{24} \text{ part/m}^3$, an inner wall density of $2.84 \times 10^{19} \text{ part/m}^3$, a maximum enrichment of 0.8293%, and a maximum depletion of 0.7085%. The enrichment of 0.8243% produces an enrichment process factor of 1.1604, or a process difference (ϵ) of 0.1604. The gas density is nearly constant at the inner wall, so that the flow rate can be at most, $1.99 \times 10^{22} \text{ part/m}^2 \text{ sec}$, since the flow must be subsonic. Assuming that the extraction withdraws a gas thickness of 1 cm from the inner wall [15], the extraction area will be 0.00346 m^2 , yielding a mass flow of $6.88 \times 10^{19} \text{ part/sec}$. For the ideal cascade, the cut should be $1/2$, so that the total flow would be $1.38 \times 10^{20} \text{ part/sec}$ or $5.43 \times 10^{-5} \text{ kg/sec}$. The separative power of the element may then be calculated

$$\begin{aligned}\delta U &= \frac{\theta}{1 - \theta} \frac{G \omega^2}{2} \\ &= \frac{0.5}{1 - 0.5} \frac{(1.38 \times 10^{20} \text{ part/sec})(0.1604)^2}{2} \\ &= 1.78 \times 10^{18} \frac{\text{part}}{\text{sec}} = 7.02 \times 10^{-7} \frac{\text{kg}}{\text{sec}}\end{aligned}$$

The separative work required to produce 0.8243% enriched uranium may be evaluated from Equation 5.23,

$$\frac{\Delta}{L} = 0.134 \frac{\text{kg SWU}}{\text{kg product}}$$

The total flow is the product of δU and Δ/L

$$\begin{aligned}\text{Flow} &= (\delta U) \frac{\Delta}{L} = (7.02 \times 10^{-7} \frac{\text{kg}}{\text{sec}}) \left(\frac{0.134 \text{ kg SWU}}{\text{kg product}} \right) \\ &= 9.41 \times 10^{-8} \frac{\text{kg SWU}}{\text{sec}} = 9.41 \times 10^{-5} \frac{\text{g SWU}}{\text{sec}}\end{aligned}$$

A gas centrifuge plant will produce about 1-10 kg of slightly enriched uranium per year [1]. If the process factor is only 1.055, the flow rate will be 1.40×10^{-5} g SWU/sec if the production is 10 kg per year. Avery and Davies [1] have proposed a cascade system with a process factor of 1.25. A gas centrifuge with a process factor of 1.25, and a production rate of 10 kg/year would produce a flow rate of 6.99×10^{-5} g SWU/sec.

The plasma centrifuge would require additional study before implementation in a cascade. As mentioned earlier, since the inner gas becomes highly enriched, and the outer gas only slightly stripped, the process gas remaining in the centrifuge will become slowly stripped of the ^{235}U fraction. The enrichment and stripping process factors

for this example are 1.1604 and 1.0034, respectively. With a cut of 0.5, the overall mole fraction of the two product streams would be 0.7663%. Since the feed gas was assumed to be only 0.711% enriched, the gas in the chamber would be depleted in ^{235}U . In a cascade system, the individual stages must remain constant in time. To maintain the process gas at a constant enrichment, the cut must be reduced from 0.5 to 0.0216. The flow rate of the stripped fraction must be about 45 times higher than the flow rate of the enriched fraction. A system with the same configuration with a cut of 0.0216 would produce a process rate of 4.78×10^{-5} g SWU/sec.

The process rate for the plasma centrifuge may be doubled by maintaining symmetry. Figure 2.3 shows that the configuration is axially symmetric. Feed gas may be injected near both end insulators and withdrawn at the center of the device. This arrangement would have the effect of doubling the flow rate while producing two identical outlet streams. This type of configuration may also help to eliminate the critical velocity phenomenon by reducing streaming to the end insulators.

The above example presents characteristic plasma centrifuge values, not the results of design optimization. Variations in the angular velocity, gas temperature, and device dimensions affect the separative power and the product flow. The plasma centrifuge cannot be optimized by consideration of the separative power alone, but rather by optimization of the product flow. Consider a system governed by the following conditions:

- 1) The system is a partially ionized plasma with constant angular velocity

- 2) The configuration is such that no inner wall exists, a gas pressure of p_0 is found at a radius of zero
- 3) The gas number density is constant at the outer wall
- 4) The enrichment at the outer wall is constant
- 5) Assume that the cut, θ , is equal to $1/2$.

For this configuration [1]

$$p(r) = p_0 \exp \left[\frac{m^w r^2}{2kT} \right] \quad (5.29)$$

$$\alpha(r) = \exp \left[\frac{\Delta M^w r^2}{2kT} \right] \quad (5.30)$$

where

$p(r)$ = gas pressure

$\alpha(r)$ = process factor

m = mass of the gas particles

ΔM = mass difference between the two uranium isotopes.

Since the gas number density is assumed to be constant at the outer wall, the mass flow rate will be a function of the pressure ratio

$$G(r) = \frac{c_1}{p(r)} \quad (5.31)$$

where c_1 is a constant of the system. The process difference is given by the following equation

$$\epsilon = \alpha(r) - 1 \quad (5.32)$$

The separative power may now be defined in terms of $p(r)$ and $\alpha(r)$

$$\delta U = \frac{\theta}{1 - \theta} \frac{G(r) \epsilon^2}{2} \quad (5.33)$$

Since θ is assumed to be $1/2$

$$\delta U = \frac{G(r) \epsilon^2}{2} \quad (5.34)$$

Substituting for $G(r)$ and ϵ

$$\delta U = \frac{c_1}{p(r)} \frac{[\alpha(r) - 1]^2}{2} \quad (5.35)$$

$$\delta U = \frac{c_2}{p(r)} [\alpha^2(r) - 2\alpha(r) + 1] \quad (5.36)$$

where $c_2 = c_1/2$. Substituting for $p(r)$ and $\alpha(r)$

$$\delta U = \frac{c_2}{p_0 e^{\left(\frac{m\omega^2 r^2}{2kT}\right)}} \left(e^{\left(\frac{2\Delta M\omega^2 r^2}{2kT}\right)} - 2e^{\left(\frac{\Delta M\omega^2 r^2}{2kT}\right)} + 1 \right) \quad (5.37)$$

First consider the change in separative power as a function of angular velocity

$$\frac{d\delta U}{d\omega} = \frac{(c_2/p_0)}{e^{\left(\frac{m\omega^2 r^2}{2kT}\right)}} \left(\frac{r^2 \omega}{2kT} \right) [(4\Delta M - 2m)e^{\left(\frac{2\Delta M\omega^2 r^2}{2kT}\right)} + (4m - 4\Delta M)e^{\left(\frac{\Delta M\omega^2 r^2}{2kT}\right)} - 2m] \quad (5.38)$$

For small values of x , $e^{2x} \approx 2e^x$. Simplifying

$$\frac{d\delta U}{d\omega} \approx \frac{(c_2/p_0)}{e^{\left(\frac{m\omega^2 r^2}{2kT}\right)}} \left(\frac{r^2 \omega}{2kT} \right) [4\Delta M e^{\left(\frac{\Delta M\omega^2 r^2}{2kT}\right)} - 2m] \quad (5.39)$$

For the naturally occurring uranium isotopes

$$\Delta M = 3m_p \quad (5.40)$$

$$m = 238 m_p \quad (5.41)$$

where m_p is the mass of a proton. Setting the derivative to zero and solving Equation 5.39

$$4\Delta M e^{\left(\frac{\Delta M \omega^2 r^2}{2kT}\right)} = 2m \quad (5.42)$$

Since the exponential term is the process factor, the minimum will occur when the process factor is about 40. For realistic process factors of about 1.25, the slope will be negative, indicating that the maximum separative power will be found as the angular velocity goes to zero.

A similar treatment may be performed for the temperature variation

$$\frac{d\delta U}{dT} = \frac{(c_2/P_0)}{e^{\left(\frac{m\omega^2 r^2}{2kT}\right)}} \left(\frac{r^2 \omega^2}{2kT^2}\right) \left[m - 2\Delta M e^{\left(\frac{\Delta M \omega^2 r^2}{2kT}\right)} \right] \quad (5.43)$$

Again setting the derivative to zero and solving

$$2\Delta M[\alpha(r)] = m \quad (5.44)$$

The slope is positive for all reasonable values of the process factor, reaching a value of zero for a process factor of about 40. The highest separative power would be found as the temperature approaches infinity. Optimizing the separative power does not produce the maximum amount of enriched material per element. The maximum separative power is found for a system as the angular velocity goes to zero. No enrichment could occur though, since no separation would occur. The system must be optimized by considering the flow of enriched uranium. The flow of enriched material may be obtained from the product of Equation 5.18 and Equation 5.23. The equation may not be solved in closed form. A detailed study is necessary to determine the maximum flow of material for the optimal configuration and plasma parameters.

This optimization example treats a very specific situation; a fixed geometry in a system displaying constant angular velocity. The system is comparable to a gas centrifuge. The analysis shows that the separative power cannot be optimized, and shows the difficulty in an optimization study on the product flow. A detailed analysis of the plasma centrifuge must also consider alternate distributions. Equations 4.25 and 4.26 show that certain distributions may be represented by a power equation, rather than an exponential equation, which will further serve to complicate the analysis.

Although the study is not complete, trends have been established. Decreasing the angular velocity from characteristic values will increase the separative power, but decrease the product flow. As the angular velocity becomes zero, the process difference becomes zero and the separative power goes to zero. A similar result is found for the temperature distribution. For characteristic centrifuge parameters, the product flow varies inversely with the separative power, and the product flow, not the separative power, must be optimized.

The example considered in this section was not for optimized centrifuge parameters. Nevertheless, the separative power and mass flow of the plasma centrifuge appear competitive with the diffusion plant and gas centrifuge. Although the discrete element appears feasible, the construction of an enrichment cascade may suffer serious limitations. The stripping process factor used in this example was only 1.0034, even lower than the process factor in the gaseous diffusion plant. Table 5.7 shows that the enrichment at the outer wall is relatively constant, even for extreme centrifugal forces.

Under normal density conditions, a large number of stages will be required to reduce the enrichment to a 0.2% tails assay. Although the plasma centrifuge provides high enrichment, the device only provides low depletion.

Power Consumption

The plasma centrifuge has been shown to produce high process factors with high mass flow rates. The final consideration in the feasibility study is the power consumption: How much energy will the device require to produce slightly enriched uranium?

This analysis of the energy consumption treats the plasma by the continuous fluid model [8, 13]. The plasma rotation is caused by the $\vec{J} \times \vec{B}$ force due to the interaction between the electric current in the gas and the axial magnetic field.

The plasma density will be determined by the neutral gas density, the degree of ionization, and the plasma velocity distribution. Since the plasma will be only partially ionized, the plasma density will be on the order of 10^{20} to 10^{22} part/m³. Since the plasma temperature will be only on the order of 10,000 K, the plasma pressure will be low

$$p = nkT \tag{5.45}$$

where

p = plasma pressure

n = plasma density

k = Boltzman's constant

T = plasma temperature.

When the system is in equilibrium, the plasma pressure will be balanced by the magnetic pressure

$$p_B = \frac{B^2}{2\mu_0} \quad (5.46)$$

where

p_B = magnetic pressure

B = magnitude of the magnetic field

μ_0 = permeability constant.

A magnetic field strength of 600 gauss could contain a singly ionized uranium plasma at 10,000 K with a density of 10^{22} part/m³.

Containment of the plasma is not the only function of the magnetic field. The plasma is placed in rotation by the crossed electric and magnetic fields. Increasing the magnetic field permits a reduction in the radial current, while maintaining the same driving force.

The power consumed in the device is given by the following expression

$$p\dot{W} = \phi J_r \quad (5.47)$$

where

$p\dot{W}$ = power consumed in the centrifuge

ϕ = ionization potential

J_r = radial electric current.

Increasing the magnetic field strength permits a reduction in the radial current and a reduction in the power consumption. This rationale is valid only until the power consumption in the coils producing the magnetic field dominates the system. Since the rotating plasmas are

less than 1 m in diameter, the devices can operate with magnetic field strengths as high as 60,000 gauss [4].

The centrifuge efficiency will also be improved by operation with a high ionization potential. The ionization potential, ϕ , determines the critical velocity of the plasma, as given by Equation 5.4 [22]. High rotational velocities produce high process factors. The ionization potential should be kept as high as possible without introducing unacceptably high power losses. Okada et al. [13] propose a value of 6.25 V for the ionization potential, and Lehnert suggests a value of 4 V [8]. This analysis will assume a value of 6 V, which produces a critical velocity of 2200 m/sec.

The electric current, \vec{J} , will be about 1.5 kA for the present generation centrifuge devices [4, 8, 13]. The energy consumption in the devices is not certain at this time. Lehnert estimates that the power consumption may be as low as 2000 W [8]. Bonnevier considers a highly ionized plasma and obtains a power consumption that is three orders of magnitude higher [8, 14]. Lehnert also cites the work of Odinstova on an argon plasma with a homopolar machine. The device has a radial current density of 10^4 A/m² with an ionization potential of about 4 V. If the device is only 0.2 m long with a radius of 0.1 m, the energy consumption must be at least 5 kW, and possibly higher, depending on the voltage drop across the sheath at the end insulators [8]. Okada et al. estimate that the power consumption will be about 27 kW for a device operating with a radial current of 1.5 kA and an ionization potential of 6.25 V [13].

Although the analyses and experimental findings appear to be conflicting, a number of similarities exist. The results indicate that the driving force is nearly constant in all the examples. Lehnert assumes that the current times the radius is only 6 A, or that the radial current is about 60 A. Okada et al. estimate the current to be 1500 A. The difference in the driving force lies in the magnitude of the magnetic field strength. Lehnert assumes a field strength of 20,000 gauss, while Okada et al. assumed a field strength of only 200 gauss. Higher magnetic fields permit reduced radial currents, and produce reduced power consumption. Operating rotating plasmas display magnetic field strengths ranging from 80 to 60,000 gauss [4]. A magnetic field strength of the magnitude considered by Lehnert is physically attainable. Similarly, a radial current of the magnitude proposed by Okada et al. is physically attainable. The two parameters must be combined to produce the maximum separation with the minimum power consumption.

The example in the previous section concluded that the plasma centrifuge could produce a flow of 9.56×10^{-5} gSWU/sec. Okada et al. assumed radial dimensions and an initial gas density similar to the values used on this analysis [13], therefore the power consumption should be about 27 kW. The power consumed per unit of product would be

$$\frac{27 \text{ kW}}{9.56 \times 10^{-5} \text{ gSWU/sec}} = \frac{8.96 \text{ kW}}{\text{kg SWU/yr}} = \frac{78,000 \text{ kWh}}{\text{kg SWU}}$$

Okada et al. estimate that the energy consumption in the gas centrifuge will be about 0.1 kW/(kg SWU/yr) or about 900 kWh/(kg SWU). The gaseous

diffusion plants currently require about 3100 kWh/(kg SWU). If the power consumption was reduced to 2 kW, the value that Lehnert calculates, the energy consumption per unit of product would be about 0.66 kW/(kg SWU/yr) or about 6000 kWh/(kg SWU).

Considerable power reductions may be realized by operating the plasma centrifuge devices continuously [13]. The degree of ionization is based on a calculation that assumes thermal equilibrium between the ions and electrons. When electrical energy is continuously supplied, the electrons become more energetic than the ions or atoms. This permits a larger current to be carried by the gas, which either increases the separation due to the increased rotational velocity, or permits a reduction in the power supply.

The example cited in this chapter provides characteristic values that were used in this analysis. Optimizing the flow rate or minimizing the energy consumption may also produce significant reductions in the energy consumption per unit of product. Minimizing the energy consumption requires consideration of the magnetic field strength and radial current. Increasing the magnetic field strength not only produces increased power consumption by the coils, but also affects the plasma behavior. Larger magnetic fields produce higher ionization and higher magnetic pressures. The increased ionization will tend to increase the gas temperature and decrease the process factor. In addition, the plasma region invariably displays the highest velocity and hence the highest process factor. As the magnetic pressure is increased, the plasma region width will be reduced, further reducing the process factor. These trends may be compensated for by increasing the region width of the two

gas regions. The energy savings found by reducing the radial current may more than offset any reduction in the process factor. An additional study is needed to determine the effect of these variations.

Finally, just as the authors disagree on the method of producing the separation, they also disagree on the results. Lehnert calculates a flow rate of 1.44×10^{-3} gSWU/sec with a power consumption per unit of product of 400 kWh/(kg SWU) [8]. Okada et al. estimate that the plasma centrifuge may produce a flow rate of 7.4×10^{-4} gSWU/sec and a power consumption of 10,000 kWh/(kg SWU).

If the plasma centrifuge consumes as much energy as is estimated by Okada et al., the device cannot compete with the gas centrifuge or the gaseous diffusion technique. Without further optimization, if the device displayed an energy consumption comparable to the value estimated by Lehnert, the plasma centrifuge could be competitive with the alternative enrichment techniques. Design optimization and experimental results are needed to adequately evaluate the device. Finally, the above results are based on a discrete centrifuge element. The problems concerning cascade construction still remain.

CHAPTER 6. PLASMA CENTRIFUGE LIMITATIONS

The plasma centrifuge can produce a high process factor with a high mass flow rate, and a low energy consumption. In the construction of a demonstration device, a number of problems may develop. The recognition of such problems prior to construction may permit design modifications rather than modification of the centrifuge device. Several authors have addressed problems with plasmas and rotating plasma devices [3, 5, 15, 16, 17]. In addition, Lehnert [4] has compiled a list of important plasma limitations in the device, including numerous instability mechanisms, heating requirements, radiation losses, and density limitations. Several of the important problems that may be encountered in the plasma centrifuge will be discussed in this chapter, including the following:

- 1) Velocity limitations
- 2) Mixing
- 3) Feed injection
- 4) Product extraction
- 5) Plasma expansion
- 6) Wall limitations
- 7) Shock formation
- 8) Operating procedures
- 9) Cascade construction.

Gas Limitations

Velocity limitations

The velocity limitations impose critical restraints on the plasma centrifuge. The critical velocity phenomenon is the primary source of

these limitations. The ions and electrons stream along the magnetic field lines in the axial direction and recombine at the end insulators [17]. The neutral particles form a wall layer at the end insulators. The layer becomes a source for the back-flux of matter to balance the flow of ions and electrons. As the slowly moving neutral particles flow back into the plasma, they become ionized in collisions with the rapidly rotating charged particles. The plasma velocity can only be increased to a specific critical value. At this point, the charged particles are producing a large number of ionizations at the end insulators, creating inhomogeneous electric fields that prevent the input of additional energy. Raising the input power merely increases the ionization and temperature, rather than accelerating the plasma.

Since the phenomenon arises near the end insulators, research has been directed at suppressing the mechanism at that point. One concept utilized a series of closely spaced magnetic rings around the plasma at the end insulators to suppress the inhomogeneous electric fields [17]. An inefficient contact between the rings and plasma prior to initiation of the phenomenon has prevented success. Modification of the plasma configuration also proved ineffective [3]. Figure 2.3 is an example of a device with an extended radial ratio. If the plasma rotates with a constant angular velocity, the plasma at the end insulators may be restricted to the critical velocity, while the extreme portions rotate at a velocity 10 times this value. Limitations in the

necked-down portion of this device prevented the gas from exceeding the critical velocity.

The analysis in Chapter 5 indicates that increasing the critical velocity increases the flow of separated material. Unless the mechanism can be suppressed, the separation can only be increased by reducing the temperature or increasing the device dimensions. The plasma temperature reductions are restricted by the requirements to maintain a partially ionized plasma. Decreasing the temperature reduces the degree of ionization and ultimately reduces the force that drives the neutral gas. Similar restraints may be imposed on the device dimensions. Increasing the dimensions may produce instabilities [4], and will increase the capital cost and power consumption, since the size of the magnetic field must be increased. The optimal method to increase the separation is to increase the plasma velocity, which is restricted by velocity limitations.

Mixing

The plasma centrifuge must display stable pressure, velocity, and density profiles at the point of extraction. Oscillations and instabilities may reduce the separation factor virtually to a value of unity. The sources of instabilities, other than feed injection and product extraction, will be discussed in this section.

The critical velocity phenomenon, in addition to restricting the velocity, also provides a source of mixing. The rapid ionization and inhomogeneous fields near the end insulators produce an isotropic flow

of material. If the ring system proposed in the previous section can suppress the fields, the mixing may be greatly reduced. In addition, the feed material may be inserted at the end insulators, so that the sources of the mixing are combined. The gas injection at the end insulators may provide sufficient momentum to reduce the streaming of the charged particles, and aid in the suppression of the critical velocity mechanism. Finally, the extraction point may be located near the center of the device, so that the instabilities may be damped out before extraction occurs.

The magnetic field containing the plasma may also be a source of instabilities. Variations in the field may induce plasma oscillations, inducing oscillations in the neutral gas. If the oscillations are large, they may compete with the centrifugal force and reduce the process factor. Variations in the magnetic field may also cause density variations as the coupling conditions switch to another point in space. Rapid changes in the field strength may cause changes in the particle density, resulting in further oscillations. The same restrictions may be imposed on the current density, since the crossed electric and magnetic fields drive the gas.

Temperature distributions may also cause mixing. As the neutral gas begins to become ionized by collisions, the temperature will rapidly increase. The higher temperature will reduce the pressure ratio and process factor, but will increase the gas pressure. The gas flow may become oscillatory as the pressure increases and decreases due to the ionization. The pressure oscillations may be transmitted axially to cause mixing near the extraction point. Since the neutral gas is

ionized by collisions with the charged particles, plasma density variations may cause temperature oscillations at any point in the device.

Changes in device configuration may also produce mixing. The separation will occur more rapidly if the neutral gas maintains a higher velocity. To decrease the time required for separation, the containment walls may approach the plasma edges, resulting in a larger plasma region with an increase in the average velocity of the neutral gas. The configuration changes may produce the same coupling, density, and temperature variations that were attributed to changes in the magnetic field.

Device Limitations

Feed injection

The injection of feed material into a plasma device has been an active field of research [4]. The feed may be injected into the plasma centrifuge as a high temperature neutral gas. This technique eliminates the problems associated with the injection of charged particles into a magnetic confinement. The injection of the feed material may still create problems with mixing and instabilities.

The feed gas will increase in temperature as it becomes ionized by collisions with the charged particles. The gas temperature must not create the pressure oscillations that were described in the previous discussion on mixing. The gas will be injected at the end insulators to combine instability points. The feed gas must not contribute to the buildup of ionized particles, which would increase the mechanism producing the critical velocity limitation.

The angle of feed injection must also be analyzed. Injection of the gas directly into the plasma region will create rapid ionization and accent the critical velocity mechanism. Conversely, injection parallel to the plasma may permit the gas to pass slowly into the plasma region. If the diffusion is too slow, the gas may not fully separate or reach equilibrium at the point of extraction. In this instance, it may be impossible to maintain an equimolar distribution along the length of the device, and the process factor may vary axially as well as radially. The feed gas can only be controlled by variation in the gas velocity, temperature, and insertion angle. Control of these parameters will be critical if the plasma centrifuge is to produce the maximum separation.

Product extraction

The removal of the separated material must not create instabilities that reduce the process factor. Research has been performed to study the extraction of the plasma fractions with probes [4, 15]. The insertion of a probe into the charged plasma creates instabilities, mixing, plasma cooling, and contamination. The partially ionized plasma centrifuge permits extraction without disturbing the plasma. The enriched fraction may be extracted from the inner gas region and the depleted fraction from the outer gas region. Instabilities may be produced at the extraction points, but oscillations should not propagate from the subsonic flow at both walls to the supersonic flow in the plasma region. Plasma disturbance should be minimized.

The extraction may still create a number of problems. The gas density at the inner wall will be low. To maintain high mass flow rates, the axial flow at this point must approach a Mach number of one. If the velocity becomes supersonic at the extraction point, a shock wave may be created that reduces or eliminates the separation.

The physical design of the probe will also be important. The probe can separate the gas fraction both by diversion of the gas stream and transverse flow due to pressure differences. The probe edge may erode since it will be in contact with the hot, corrosive uranium gas. This deterioration will cause mixing, reduce performance, and contaminate the uranium gas. Reliance on pressure gradients for the gas extraction requires accurate control of the pressure and flow rate to prevent supersonic flow at the extraction point.

The symmetry of the plasma centrifuge will permit the removal of two product streams. Although this technique will double the mass flow rate, it may also create additional problems. The gas will maintain an axial flow past the extraction points and the two streams will collide at the center of the device. The mass flow rate and velocity must be controlled so that the instability is minimized at that point. Mixing at the center of the device may propagate to the extraction points and reduce or eliminate separation.

Plasma expansion

Figure 2.3 shows that the radial current carried by the plasma flows from an inner anode to an exterior cathode, both of which are in contact with the plasma. As the plasma begins to rotate, the combined

effect of the repulsive forces of the charged particles and the centrifugal forces due to the rotating gas cause the plasma to expand radially.

Expansion of the plasma causes contact with the cathode plate and possibly with a boundary wall, scraping off a portion of the plasma. The expansion phenomenon results in plasma losses, cooling, contamination, and mixing. Variations in the magnetic field, in the coupling locations, or in the density distributions may cause increased plasma expansion. The mixing created by the plasma-wall interactions may cause serious reductions in the process factor.

Wall limitations

The containment walls will be exposed to conditions ranging from large pressure gradients to radiation damage. The walls need not meet the stringent requirements of a fusion device. The plasma density and temperature are low so that radiation losses are small. The plasma density near the wall should be low so that the erosion caused by plasma streaming will be small. The shear force at the wall will also be low since the rotational velocity goes to zero at that point.

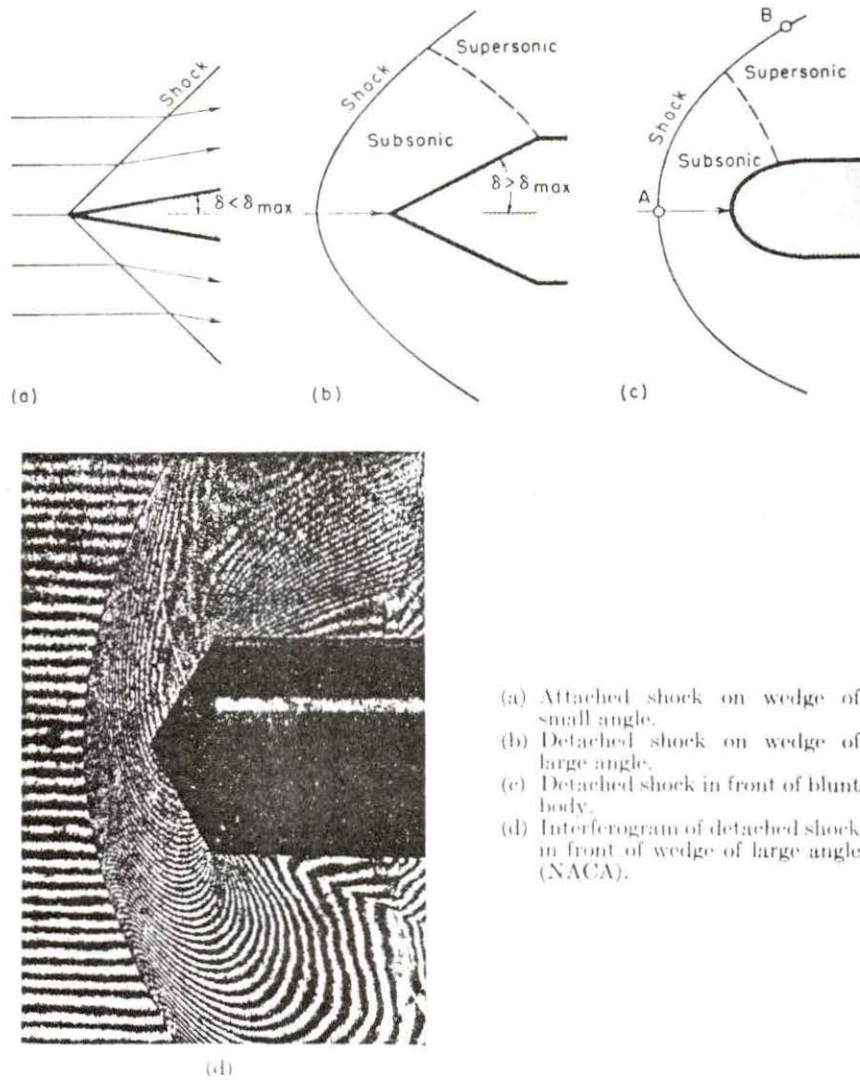
The primary wall limitations will be due to containment of the uranium gas. The inner wall must withstand a relatively high vacuum. A gas at 10,000 K with a density of 10^{19} part/m³ will exert a pressure of about 10^{-5} atm. The outer wall must withstand a high pressure. A gas at the same temperature with a density of 5×10^{24} part/m³ will exert a pressure of nearly 7 atm. The walls must also withstand corrosion from the hot uranium gas. The walls are limited in thickness

and type of material since the coils creating the magnetic field must be exterior to the wall. The walls must also conform to the plasma configuration with a high degree of precision. The material must be easily machined to produce the close tolerances required for high separation. The wall material must also be easily worked and sealed since penetrations must be made for the insertion and extraction probes.

Shock formation

The plasma centrifuge produces high velocity, three-dimensional flow. The flow in the plasma region may be in excess of Mach 5 while the flow at the walls must be subsonic. As the gas slows toward the boundary walls, a shock wave may form. A shock wave is characterized by a rapid pressure increase and velocity decrease over a very small distance. The pressure and velocity changes can occur in a thickness on the order of 10^{-5} cm, comparable to the mean free path of the gas [23].

The pressure and velocity discontinuities are inclined in the direction of flow. The three-dimensional flow will produce an oblique shock wave rather than the normal shock encountered in one-dimensional flow. Although oblique shock waves occur in almost all supersonic flow patterns, the presence of supersonic flow does not require the presence of shock waves [23]. If a shock wave does form, the shock may be attached to a flow surface or the shock may be detached. Figure 6.1 shows the effect of attached and detached shocks. The velocity profile in the plasma centrifuge can produce an oblique shock at any point in the configuration where the flow is supersonic. Although the extraction



- (a) Attached shock on wedge of small angle.
- (b) Detached shock on wedge of large angle.
- (c) Detached shock in front of blunt body.
- (d) Interferogram of detached shock in front of wedge of large angle (NACA).

Fig. 6.1. Attached and detached shock [23].

probe may be in the subsonic flow pattern, a detached shock could still form in the supersonic flow region.

Figure 6.1 shows that a shock wave may be formed by an obstruction. A protruding containment wall, extraction probe, or plasma cathode would be an example of such an obstruction. The obstructions must be located in the subsonic flow to prevent the shock formation. Nevertheless, an oblique shock wave may still occur due to changes in the device parameters. Rapid changes in the gas temperature or density may induce the shock. Pressure oscillations, as described for the feed gas ionization, may also induce shock waves.

The effect of the shock wave is uncertain. The rapid pressure and velocity variations across the shock may produce oscillations and mixing in the gas. Figure 6.2 shows the instabilities produced by shock waves as the fluid strikes the obstruction at Mach 3.6. It may be possible to create the shock wave some distance before extraction so that the flow will be stable at the point of extraction. Due to the different pressure distributions for the two isotopes, the shock wave may actually increase separation, since one isotope may penetrate the shock more easily than the other. If the shock decreases the separation, the extent of the reduction must be evaluated.

Operating procedures

Optimum design parameters may be difficult to maintain in the plasma centrifuge. Operation at specified parameters may not be possible. For example, while the optimal separation may occur at a temperature of 8,000 K, oscillations in the feed flow may occur that

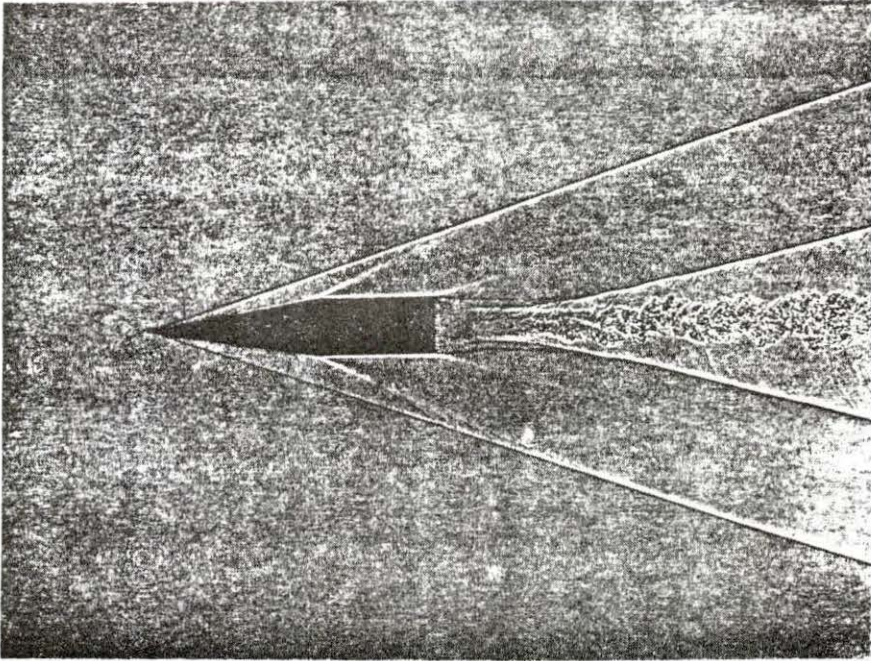


Fig. 6.2. Turbulence following an obstruction in a supersonic flow pattern [24].

produce temperature oscillations or mixing. Operation at 10,000 K could reduce the oscillations, but require operation under less than ideal conditions. The plasma centrifuge performance is dependent on feed gas conditions, magnetic field strength, radial current, gas density and temperature, plasma temperature and density, and the plasma velocity distribution. Since several of the above parameters are related, optimization and operation at the optimal conditions may be difficult to maintain.

Cascade construction

Uranium enrichment plants to supply the present generation of light water reactors produce a product stream of 2-4% ^{235}U and a waste stream of 0.2% ^{235}U . The plasma centrifuge may be limited due to the differences in process factors and due to the difficulty of connecting the centrifuge elements.

The plasma centrifuge may produce an enrichment process factor of about 1.20, but the stripping process factor will be less than 1.0040. Given natural uranium feed with 0.711% ^{235}U , 8 stages would be required to enrich the feed to 3% ^{235}U while 318 stages would be required to deplete the feed to 0.2% ^{235}U , using the stripping and enrichment process factors from above. A plasma centrifuge element will consume more energy than a diffusion element, making depletion economically uncompetitive. In addition, the design of the cascade will also be difficult. In the gaseous diffusion plant, the stripping and enrichment process factors are the same value, permitting separation by only one element. If the stripping and enrichment process factors are 1.004 and

1.20 respectively, over 40 stages are required to deplete the gas to an enrichment where the product stream returns to the original enrichment. The large difference between the process factors will require that the device operate with a low cut. To maintain a constant molar concentration in the centrifuge, the flow rate of the stripped fraction may be 40 times higher than the flow rate of the enriched fraction, requiring the processing of a large volume of material.

The plasma centrifuge may also present problems in the construction of the cascade. The discussion on feed injection indicated that the gas temperature, velocity, and angle of injection must be controlled to prevent instabilities and mixing. If the preceding stage does not produce these parameters, additional equipment must be supplied to modify the gas flow. The process equipment to connect the centrifuge elements could be costly, complicated, and expensive to operate.

CHAPTER 7. FUTURE WORK

Throughout this analysis, a number of important research areas have been identified. This chapter will consider the research in two specific areas; the measurement of device parameters and additional design analysis.

Measurement of Parameters

A detailed analysis of the plasma centrifuge cannot be completed until specific physical distributions are measured. This section will discuss the parameters and their importance in the plasma centrifuge. The following section will consider additional analysis work.

Plasma limitations

Lehnert has shown that a partially ionized plasma can place a neutral gas in rotation [6]. To optimize the device, several plasma limits must be established:

- 1) Minimum temperature required to maintain a stable plasma
- 2) Minimum degree of ionization to maintain a stable plasma
- 3) Maximum pressure variation
- 4) Minimum radial current density
- 5) Maximum neutral gas density
- 6) Maximum drag force that still permits rotation
- 7) Minimum power requirement.

Coupling requirements

Lehnert has derived requirements governing the coupling between the plasma and the neutral gas. For specific density, temperature, and velocity requirements, the neutral gas will conform to the plasma velocity distribution in the plasma region. The coupling conditions determine the gas velocity and ultimately determine the density distribution and device performance. Research is necessary to determine the location of these regions and the validity of these predictions.

Plasma velocity profile

Three velocity distributions in the plasma were considered in this analysis. Figure 5.2 shows the effect of the distribution on the process factor. The plasma velocity distribution must be evaluated to predict the device performance.

The determination of the plasma velocity profile is complicated by the relationship between the plasma density and plasma velocity. The rotating plasma will produce a centrifugal force that drives the particles to the outer wall, making the plasma density dependent on the velocity profile. But the velocity profile itself is dependent on the plasma density [8].

The plasma density distribution and plasma velocity distribution must be known to determine the coupling conditions. The coupling points determine the width of the gas regions, and the velocity distribution in those regions. The process factor and pressure ratio are both strong functions of the gas velocity and region width. Ultimately,

the plasma density and velocity must be measured to predict the device performance.

Temperature distribution

The pressure ratio and process factor have also been shown to be a strong function of the gas temperature. The feed gas temperature may increase as the neutral gas becomes ionized by collisions with charged particles in the plasma. The gas temperature may be found to be highest in the plasma region and decreasing toward the walls. Due to ionizations, the gas temperature should conform to the plasma density distribution in the plasma region. An accurate temperature mapping across the configuration is required to evaluate the centrifuge performance.

Shock formation

The effect of a shock wave on the plasma centrifuge must also be measured. The majority of research on oblique shocks has been performed on the effect of a projectile or obstruction in supersonic flow; conditions found in ballistics work and aerospace research [22, 23]. The shock in this instance may be unattached in a supersonic or hypersonic flow region. In addition, the gas will be at a high temperature and possibly a low density, such as the conditions found at the inner wall. The centrifuge must be studied to determine if a shock wave will form. If a shock is detected, the device must be further analyzed to determine the effect of the shock and system variations that may eliminate the shock or reduce the effect.

Pressure variation

The plasma centrifuge predicts large pressure ratios, with a low gas density at the inner wall. The pressure ratio must vary slowly over a mean free path of the gas. Near the inner wall, this condition is not met. This requirement may cause an increase in the gas density at the inner wall. The lighter gas fraction will have a higher probability of being found at that point, so that the separation may increase. The increased density could produce a higher flow rate. The increased process factor and higher flow rate would increase the separative power of the element and reduce the power consumption. Additional study in the field of high temperature, low density thermodynamics is required.

Design Analysis

In addition to the measurement of parameters, theoretical studies may also provide information about the plasma centrifuge. For example, it may be found that the plasma will maintain some velocity distribution at a particular density. An analysis may predict that a larger magnetic field would produce a more dense plasma and provide a higher separative power. This section discusses several areas that require additional study.

Optimization

Research is needed to determine the parameters that produce the maximum flow of enriched material. The discussion in Chapter 5 indicated that the flow, rather than the separative power, must be

optimized. Increasing the region width, increasing the critical velocity, and decreasing the temperature increase the process factor and pressure ratio. Since the pressure ratio increases more rapidly than the process factor, the separative power decreases as the process factor increases. The total flow increases to a maximum value and finally decreases. The trend has been established, but a detailed analysis is required to determine the optimal configuration and parameters to produce the maximum separation.

Extraction study

Flow in the radial direction was neglected in this study. The extraction of gas may superimpose a radial velocity component on the gas distribution. An extraction study is needed to evaluate the magnitude of the radial velocity component, and the effect of this velocity component on the process factor.

Three-dimensional study

The analysis in this study was performed in a two-dimensional cylindrical coordinate system with no flow in the axial or radial direction. When considering a mass flow, the configuration must be analyzed for both the axial and radial velocity profile.

The gas pressure ratio must be evaluated by an iterative calculation over the configuration. The plasma velocity and pressure distribution must first be obtained. A neutral gas density distribution may then be assumed. The gas will produce coupling at points determined by the constraints predicted by Lehnert [8]. Since the total number of particles in the device are known, the density may be integrated

numerically across the configuration to check the assumption. The total number of particles may be checked against the assumption to test the distribution. The axial velocity may then be superimposed on the density distribution. The radial velocity profile must be further imposed on this profile, with the constraint that the velocity must be subsonic at the extraction point.

Flow constraints

The plasma centrifuge requires a finite time to separate the light and heavy fractions of the gas. Okada et al. [13] have described the separation time by a time constant measuring the ratio of the buildup of the gas momentum to the driving force. The separation time may be reduced by increasing the average gas velocity. Since the gas velocity is highest in the plasma region, the average gas velocity may be increased by expanding the width of the plasma region. The region width may be changed by variations in the gas density, variation in the magnetic field strength, or variations in the boundary wall configuration. A study of the flow system is required to determine the flow rate that provides the maximum separation in the dimensions of the device.

Wall configuration

Variations in the wall configuration may produce spatial variations in the coupling points. Changes in the coupling location may induce oscillations in the gas and reduce the separation. The wall configuration may be changed in order to increase the process factor or decrease the separation time. A complete analysis must be performed

to map the coupling points in the axial direction. The study will indicate variations that may occur due to density changes, and will determine the location of any discontinuities.

Mode of operation

The plasma centrifuge must be analyzed to determine the optimal mode of operation. The device may be operated in a number of different ways; including pulsed operation, continuous operation, and oscillatory operation. The method of pulsed operation may produce good separation with a low energy consumption. Several of the existing rotating plasma devices operate in this mode. The gas may not reach equilibrium, which will reduce the process factor, but will increase the mass flow rate since the fully developed pressure distribution will not form.

Okada et al. [13] estimate that higher separation can be achieved by continuous, rather than pulsed operation. Higher electron energies will improve the gas conductivity permitting higher current densities with the same power consumption. The plasma centrifuge may also be operated in an oscillatory mode. A plasma centrifuge operating continuously could be pulsed at the inner wall with a jet of feed material. The pulse would create a pressure wave moving toward the plasma edge. The increased density could move the coupling point closer to the inner wall, increasing the pressure ratio and process factor. When the pressure wave passed and the system returned to equilibrium, the lighter fraction will diffuse to the inner wall more rapidly than the heavy fraction. The pulse could be repeated to develop higher

enrichments at the inner wall. The analysis of these modes of operation or other alternatives is required to optimize the centrifuge performance.

Cascade configuration

The analysis of the plasma centrifuge will not be complete until the elements are arranged in a cascade. The centrifuge produces different process factors for enrichment and stripping. The difference in the process factors prevents the construction of an ideal cascade and requires a cut considerably less than $1/2$. This difference, coupled with the low depletion in the stripped fraction may make the cascade difficult to design.

Economic analysis

An economic analysis must also be performed to estimate the cost of the product. The capital cost may be estimated by consideration of the equipment needed to produce the uranium gas, the equipment for the extraction, and the process equipment to transfer the product from one stage to the next. The operating cost may be estimated from the energy consumption and the value of the waste material.

CHAPTER 8. CONCLUSION

The plasma centrifuge is a hybrid between the gas centrifuge and calutron. Theoretically, the technique offers a number of advantages over alternative enrichment methods; including large rotational velocities, low wall interactions, and the elimination of moving mechanical parts.

Initial investigations and experiments on rotating plasmas indicate that a low temperature plasma may be placed in rotation by crossed electric and magnetic fields. The neutral gas exerts a drag force on the plasma and this force in turn places the neutral gas in rotation. This work continues the analysis by assuming that the plasma divides the neutral gas into three regions, a plasma region and two gas regions. The neutral gas particles in the plasma region will be coupled to the plasma under certain density constraints. The gas will conform to the plasma velocity distribution under these conditions. Continuity of the gas parameters determines the boundary conditions and ultimately the velocity distribution in the two gas regions.

The rotating gas is composed of the two naturally occurring uranium isotopes. The centrifugal forces created by the rotating gas drive the heavier fraction to the outer wall while the lighter fraction is driven to the inner wall. The variations in gas density produce changes in the gas pressure and enrichment across the centrifuge device. Changes in the velocity distribution, critical velocity, temperature, and device dimensions produced the following results.

1) Process factors on the order of 1.20 are predicted. The highest process factors will be found in the region of highest velocity.

2) Larger region widths produce higher process factors.

3) The process factor may be increased by decreasing the temperature or increasing the critical velocity.

4) Regardless of the plasma velocity distribution, large enrichment process factors may be predicted by the proper section of temperature, centrifuge dimensions, and critical velocity.

5) Variations in plasma parameters produce changes in the inner wall number density of 15 orders of magnitude, while changing the outer wall density by only a factor of 2.

6) Different enrichment and stripping process factors are produced. While the enrichment process factor may be in excess of 1.2, the stripping process factor is only on the order of the gaseous diffusion plant, about 1.004. This difference may cause significant problems in the cascade design.

7) The plasma centrifuge elements cannot be arranged in an ideal cascade due to the difference between the stripping and enrichment process factors. If the cut is maintained at 1/2, the gas in the element will be continually depleted in the lighter gas fraction.

8) A large number of stages will be required to deplete the uranium to the traditional 0.2% tails assay. Since the stripping process factor is lower than that found in the diffusion plant, even more stages will be required and the energy consumption will be more intense.

9) The energy consumption per unit of product may be competitive with alternative enrichment schemes if the magnetic field strength and radial current are properly chosen.

10) Extraction will be restricted to a narrow region near the inner and outer wall in order to prevent the formation of an oblique shock in the supersonic flow near the plasma region. This condition necessarily restricts the axial flow rate.

11) The pressure ratio increases more rapidly than the process factor. Increasing the critical velocity or decreasing the temperature reduces the separative power. The total flow, in (kg SWU/sec), rather than the separative power, must be optimized for the plasma centrifuge.

12) The mixing produced by gas injection and extraction should be minimized by the proper selection of the flow rate, position, and flow angle.

13) Temperature and velocity variations may perturb the system.

Additional experimentation is needed to evaluate these effects. Considering the enrichment stages alone, the plasma centrifuge appears competitive with alternative enrichment schemes. Adjustments in gas density, temperature, device dimensions, or critical velocity predict a gas distribution with a separative power in excess of both the diffusion technique and gas centrifuge. The power consumption may be higher, but reductions in the capital cost and system complexity may make the product more economical.

A competitive enrichment scheme must not only enrich the product stream, but must also deplete the waste stream. The process factor for the stripped fraction in present generation centrifuge devices is so

low that a large number of stages, and subsequently high energy consumption, would be necessary to deplete the gas to the traditional tails assay. Although the plasma centrifuge can enrich the uranium in a small number of stages, the device cannot deplete the feed. A cascade system similar to that used in the gaseous diffusion plants could not be constructed.

The device may be practical for enrichment purposes alone. The plasma centrifuge could be used to produce highly enriched uranium. Alternatively, the device could be used in an enrichment scheme whereby the centrifuge would enrich the gas and an alternative method would deplete the gas. Future modifications may permit the construction of devices with extended axial dimensions. This would permit diffusion between the enriched and depleted fractions, possibly increasing the process factors to the point that stripping would become competitive in the plasma centrifuge. Although the discrete elements appear feasible, the existing plasma centrifuge designs are not acceptable for a complete enrichment scheme.

REFERENCES

1. Avery, D. G., and E. Davies. 1973. Uranium enrichment by gas centrifuge. Mills & Boon Limited, London, England (Distributed in the United States by Crane, Russak & Company, Inc., New York, New York). 96 pp.
2. Becker, E. W., W. Bier, W. Ehrfeld, K. Shubert, R. Schuette, and D. Seidel. 1975. Uranium enrichment by separation nozzle processes. American Nuclear Society, Trans. 22: 313-314.
3. Lehnert, B. 1974. On the equilibrium and stability of rotating high-beta plasmas. Physica Scripta 9: 229-236.
4. Lehnert, B. 1971. Rotating plasmas. Nuclear Fusion 11: 485-533.
5. Uman, Martin A. 1964. Introduction to plasma physics. McGraw-Hill, New York, New York. 226 pp.
6. Lehnert, B. 1970. A partially ionized plasma centrifuge. Physica Scripta 2: 106-107.
7. Sabri, Z. 1974. Uranium enrichment using plasma centrifuges. American Nuclear Society, Trans. 19: 230.
8. Lehnert, B. 1973. The partially ionized plasma centrifuge. Physica Scripta 7: 102-106.
9. Forsen, H. K., G. S. Janes, and R. H. Levy. 1975. Prospects for uranium laser isotope separation. American Nuclear Society, Trans. 22: 312-313.
10. Snavely, B. B. 1975. Isotope separation using tunable lasers. (CONF-750627-1). USERDA Technical Information Center, Oak Ridge, Tenn. 14 pp.
11. Ferguson, A. T. 1975. International conference on uranium isotope separation. Journal of the British Nuclear Energy Society 14: 213-219.
12. Weast, Robert C., editor. 1970. Handbook of chemistry and physics. 51st ed. The Chemical Rubber Co., Cleveland, Ohio. 2364 pp.
13. Okada, Osami, Taro Dodo, and Toshio Kawai. 1973. Separation of uranium isotope by plasma centrifuge. Journal of Nuclear Science and Technology 10: 626-631.
14. Bonnevier, B. 1966. Diffusion due to ion-ion collisions in a multicomponent plasma. Arkiv För Fysik 33: 255-270.

15. Bonnevier, B. 1970. Experimental evidence of element and isotope separation in a rotating plasma. *Plasma Physics* 13: 763-774.
16. Brahme, A. 1970. On the hydromagnetic stability of a nonuniformly rotating fluid. *Physica Scripta* 2: 108-112.
17. Lehnert, B. 1974. On the possibilities of plasmas rotating at super-critical velocities. *Physica Scripta* 9: 189-192.
18. Lehnert, B., J. Bergström, S. Holmberg, and B. Wilner. 1970. On the interaction between a fully ionized plasma and a neutral gas blanket. *Physica Scripta* 1: 39-45.
19. Welty, James R., Charles E. Wicks, and Robert E. Wilson. 1969. Fundamentals of momentum, heat and mass transfer. John Wiley & Sons, Inc., New York, New York. 697 pp.
20. Cohen, Karl. 1951. The theory of isotope separation. McGraw-Hill, New York, New York. 165 pp.
21. Sesonske, Alexander. 1973. Nuclear power plant design analysis. TID-26241. (Technical Information Center, Office of Information Services, U.S. Atomic Energy Commission.)
22. Alfvén, H. 1954. On the origin of the solar system. Clarendon Press, Oxford, England. 194 pp.
23. Shapiro, Asher H. 1954. The dynamics and thermodynamics of compressible fluid flow. Ronald Press Co., New York, New York. 2 vols.
24. Binder, Raymond C. 1973. Fluid mechanics. 5th ed. Prentice-Hall, Inc., Englewood Cliffs, N.J. 393 pp.

ACKNOWLEDGMENTS

The author is indebted to his major professor, Dr. Zeinab Sabri, for the valuable discussions and guidance offered in the completion of this study. In addition, the author is further indebted to the U.S. Energy Research and Development Administration for funding this work. Finally, a special thanks are directed to Vicki, for the encouragement and understanding given throughout this study.

APPENDIX A. PROGRAM LISTING

```

$JOB 'J',TIME=60,PAGES=65
1     REAL RWI,RPI,RPO,RWO,OMEG,ANGI,ANG,BOLT,T,I,DELL,V,PR,M,MP,ALFA
2     REAL CONV,TEST,ITER,DEN,NINT
3     REAL PRNOT,PROLD,NNOT,PRTOT,NAV,NW,NTOT,PRIT,PRNEW
4     REAL N,PI,ALF,U,UMAX,NMAX,NINC,NTEST,RAV,R,ORIG,INC
5     REAL X,MX,NPOT,PPOLD,PP,PPTOT,PPNEW,PPIT,NPV,NPNT,NWX,NWZ,F,ENR
6     REAL CONST,OMEGI,OMEGO
7     COMMON PR,PP,ANG,V
8     1   FORMAT (16I5)
9     2   FORMAT (16F5.3)
10    3   FORMAT (8F10.5)
11    READ (5,1) NSETS
12    NS=0
13    5   CONTINUE
C
C     INPUT VARIABLES
C     NSETS (NUMBER OF SETS), RWI (RADIUS OF INNER WALL), RPI (RAD-
C     IJS OF INNER PLASMA EDGE), RPO (RADIUS OF OUTER PLASMA EDGE),
C     RWO (RADIUS OF OUTER WALL), OMEG (PLASMA CRITICAL ANGULAR
C     VELOCITY AT 0.1 M), T (TEMPERATURE), IOPT (OPTION FOR PLASMA
C     DISTRIBUTION)
C     DELL (INCREMENTAL SPACING), PROLD NNOT PPOLD NPOT END (INITIAL-
C     IZE PARAMETERS)
C     F (FEED U235 FRACTION), PI (CONSTANT PI), MP (MASS OF THE
C     PROTON), NTOT (TOTAL NUMBER OF PARTICLES)
C
14    READ(5,10) RWI,RPI,RPO,RWO,OMEG,T,IOPT
15    10  FORMAT (6F10.4,I5)
16    READ(5,2) DELL,PROLD,NNOT,PPOLD,NPOT,END
17    READ (5,3) F,PI,MP,NTOT
18    WRITE(6,20)

```

```

19      20  FORMAT ('1',50X,'INPUT DATA',/,/,10X,'RWI',10X,'RPI' ,10X,'RPO',10X
      C,'RWO',10X,'OMEG',12X,'T',10X,'DELL',/)
20      WRITE(6,30) RWI,RPI,RPO,RWO,OMEG,T,DELL
21      30  FORMAT (' ',7X,F7.3,6X,F7.3,6X,F7.3,6X,F7.3,6X,F8.1,8X,F7.0,6X,
      CF7.4)
22      K=0
23      I=RWI
24      M=238./6.023E 26
25      MX=235./6.023E 26
26      BOLT=8.61E-5
27      CONV=1.602E-19

      C
      C  DETERMINE CONSTANTS FOR EACH OPT IGN
      C
28      IF (IOPT.EQ.0) GO TO 1000
29      IF (IOPT.EQ.1) GO TO 1100
30      WRITE (6,1200)
31      1200 FORMAT (' ',/,/,5X,'*****CONSTANT ACCELERATION*****',/)
32      CONST=OMEG*0.1**2
33      OMEGI=CONST/RPI**2
34      OMEGO=CONST/RPO**2
35      GO TO 2000
36      1000 WRITE (6,1010)
37      1010 FORMAT (' ',/,/,5X,'*****CONSTANT ANGULAR VELOCITY*****',/)
38      CONST=OMEG
39      OMEGI=OMEG
40      OMEGO=OMEG
41      GO TO 2000
42      1100 WRITE (6,1110)
43      1110 FORMAT (' ',/,/,5X,'*****CONSTANT TANGENTIAL VELOCITY*****',/)
44      CONST=OMEG*0.1
45      OMEGI=CONST/RPI
46      OMEGO=CONST/RPO
47      2000 CONTINUE

      C
      C  CALCULATE PRESSURE RATIO TO EVALUATE WALL PRESSURE AND DENSITY
      C

```



```

48      WRITE(6,2210)
49      2210 FORMAT(' ',/,30X,'PRESSURE DATA',/,10X,'PRTOT', 10X, 'NUMBER OF P
        CARTICLES', 10X,'U235 WALL DEN',10X,'U238 WALL DEN'./)
50      2220 IF(I.LT.RPI) GO TO 2240
51      IF(I.LT.RPU) GO TO 2250
52      Z=M* OMEGO**2/BOLT/T/CONV
53      X=MX* OMEGO**2/BOLT/T/CONV
54      PR=EXP(RPO**4*Z/(RWO**2-RPO**2)**2*((I**2-RPO**2)/2.-2.*RWO**2*ALO
        CG(I/RPO)+RWO**4/2.*(1./RPO**2-1./I**2)))
55      PP=EXP(RPU**4*X/(RWO**2-RPO**2)**2*((I**2-RPO**2)/2.-2.*RWO**2*ALO
        CG(I/RPO)+RWO**4/2.*(1./RPO**2-1./I**2)))
56      PRTOT=PR*PRNEW
57      PPTOT=PP*PPNEW
58      GO TO 2260
59      2240 CONTINUE
60      Z=M* OMEGI**2/BOLT/T/CONV
61      X=MX* OMEGI**2/BOLT/T/CONV
62      PR=EXP(RPI**4*Z/(RPI**2-RWI**2)**2*((I**2-RWI**2)/2.-2.*RWI**2*
        C ALOG(I/RWI) + RWI**4/2.*(1./RWI**2-1./I**2)))
63      PP=EXP(RPI**4*X/(RPI**2-RWI**2)**2*((I**2-RWI**2)/2.-2.*RWI**2*
        C ALOG(I/RWI) + RWI**4/2.*(1./RWI**2-1./I**2)))
64      PRTOT=PR
65      PRIT=PR
66      PPTOT=PP
67      PPIT=PP
68      GO TO 2260
69      2250 CONTINUE
70      Z=M* CONST**2/BOLT/T/CONV
71      X=MX* CONST**2/BOLT/T/CONV
72      IF (IOPT.EQ.0) CALL CONDMG(I,RPI,Z,X,CONST)
73      IF (IOPT.EQ.1) CALL CONVEL(I,RPI,Z,X,CONST)
74      IF (IOPT.EQ.2) CALL CONACC(I,RPI,Z,X,CONST)
75      PRTOT=PR*PRIT
76      PRNEW=PRTOT
77      PPTOT=PP*PPIT
78      PPNEW=PPTOT

```

```

79     2260 NAV=( PROLD + PRTOT)/2.
80     NPV=( PPOLD + PPTOT)/2.
81     A=2.*PI*(I-DELL/2.)*DELL
82     NINT=NNOT + NAV*A
83     NNOT=NINT
84     NPNT=NPOT + NPV*A
85     NPOT=NPNT
86     I=I+DELL
87     IF (I.LT.RWD) GO TO 2220
88     NWX=F*NTOT/NPNT
89     NWZ= (1.-F)*NTOT/NINT
90     WRITE(6,2280)PRTOT,NTOT,NWX,NWZ
91     2280 FORMAT(' ',4X, E12.4,10X, E12.4,14X,E12.4, 10X, E12.4)
C
C     EVALUATE VELOCITY, PRESSURE, DENSITY, AND ENRICHMENT DISTRIBUTIONS
C     ACROSS THE CONFIGURATION
C
92     I=RWI
93     READ(5,2) DELL,PROLD,NNOT,PPOLD,NPOT,END
94     WRITE(6,2300)
95     2300 FORMAT(' ',//,50X,'GAS DATA',/,5X, 'RADIUS',5X, 'ANG VEL',5X, 'VEL
COCITY', 5X,'PRESSURE RATIO ',5X,'PRES RATIO TOT ',7X,'DENSITY', 7X,
C 'PROCESS FACTOR',5X,'ENRICHMENT',/)
96     2310 IF (I.LT.RPI) GO TO 2340
97     IF (I.LT.RPO) GO TO 2350
98     X=MX* OMEGO**2/BOLT/T/CONV
99     Z=M*  CMEGO**2/BOLT/T/CONV
C     OUTER REGION
100    V= RPO**2*OMEGO/( RWO**2 - RPO**2)*(RWO**2/I-I)
101    ANG=V/I
102    PR=EXP(RPO**4*Z/(RWO**2-RPO**2)**2*((I**2-RPO**2)/2.-2.*RWO**2*ALO
CG(I/RPO)+RWO**4/2.*(1./RPO**2-1./I**2)))
103    PP=EXP(RPO**4*X/(RWO**2-RPO**2)**2*((I**2-RPO**2)/2.-2.*RWO**2*ALO
CG(I/RPO)+RWO**4/2.*(1./RPO**2-1./I**2)))
104    PRTOT=PR*PRNEW
105    PPTOT=PP*PPNEW
106    GO TO 2360

```

```

C          INNER REGION
107 2340 V=RPI**2* OMEGI / (RPI**2 - RWI**2)*(I-RWI**2/I)
108      Z=M* OMEGI**2/BOLT/T/CONV
109      X=MX* OMEGI**2/BOLT/T/CONV
110      ANG=V/I
111      PR=EXP(RPI**4*Z/(RPI**2-RWI**2)**2*((I**2-RWI**2)/2.-2.*RWI**2*
C      ALOG(I/RWI) + RWI**4/2.*(1./RWI**2-1./I**2)))
112      PP=EXP(RPI**4*X/(RPI**2-RWI**2)**2*((I**2-RWI**2)/2.-2.*RWI**2*
C      ALOG(I/RWI) + RWI**4/2.*(1./RWI**2-1./I**2)))
113      PRTOT=PR
114      PRIT=PR
115      PPTOT=PP
116      PPIT=PP
117      GO TO 2360
C          PLASMA REGION
118 2350 CONTINUE
119      Z=M* CONST**2/BOLT/T/CONV
120      X=MX* CONST**2/BOLT/T/CONV
121      IF (IOPT.EQ.0) CALL CONOMG(I,RPI,Z,X,CONST)
122      IF (IOPT.EQ.1) CALL CONVEL(I,RPI,Z,X,CONST)
123      IF (IOPT.EQ.2) CALL CONACC(I,RPI,Z,X,CONST)
124      PRTOT=PR*PRIT
125      PRNEW=PRTOT
126      PPTOT=PP*PPIT
127      PPNEW=PPTOT
C
C      CALCULATE DENSITY, ENRICHMENT, AND PROCESS FACTOR
C
128 2360 CONTINUE
129      K=K+1
130      NPNTS=K
131      DEN= PRTOT*NWZ + PPTOT*NWX
132      ENR= PPTOT*NWX/(PRTOT*NWZ + PPTOT*NWX)
133      IF (ENR.GT.ENQ) ENO=ENR
134      ALFA= (1.-ENR) / ENR*ENO / (1.-ENO)

```

```

135      WRITE(6,2380)I,ANG,V,PR,PRTOT,DEN,ALFA,ENR
136      2380 FORMAT (' ',4X, F7.5,5X, F7.1,6X, F7.1, 5X, E12.4,7X,E12.4,7X,
      C E12.4, 7X, F8.6,8X, F8.6)
      C      OUTPUT VARIABLES
      C      I (POSITION), ANG (ANGULAR VELOCITY), V (ROTATIONAL VELOCITY)
      C      PR (PRESSURE RATIO, BY REGION), PRTOT (TOTAL PRESSURE RATIO),
      C      DEN (GAS NUMBER DENSITY), ALFA (SIMPLE PROCESS FACTOR), ENR
      C      (ENRICHMENT)
137      I=I+DELL
138      IF (I.LT.RWO) GO TO 2310
139      NS=NS+1
140      IF (NS.LT.NSETS) GO TO 5
141      STOP
142      END

      C
      C      SUBROUTINES
      C      CONOMG (CONSTANT ANGULAR VELOCITY)
      C      CONVEL (CONSTANT ROTATIONAL VELOCITY)
      C      CONACC (VELOCITY*RADIUS = CONSTANT)
      C

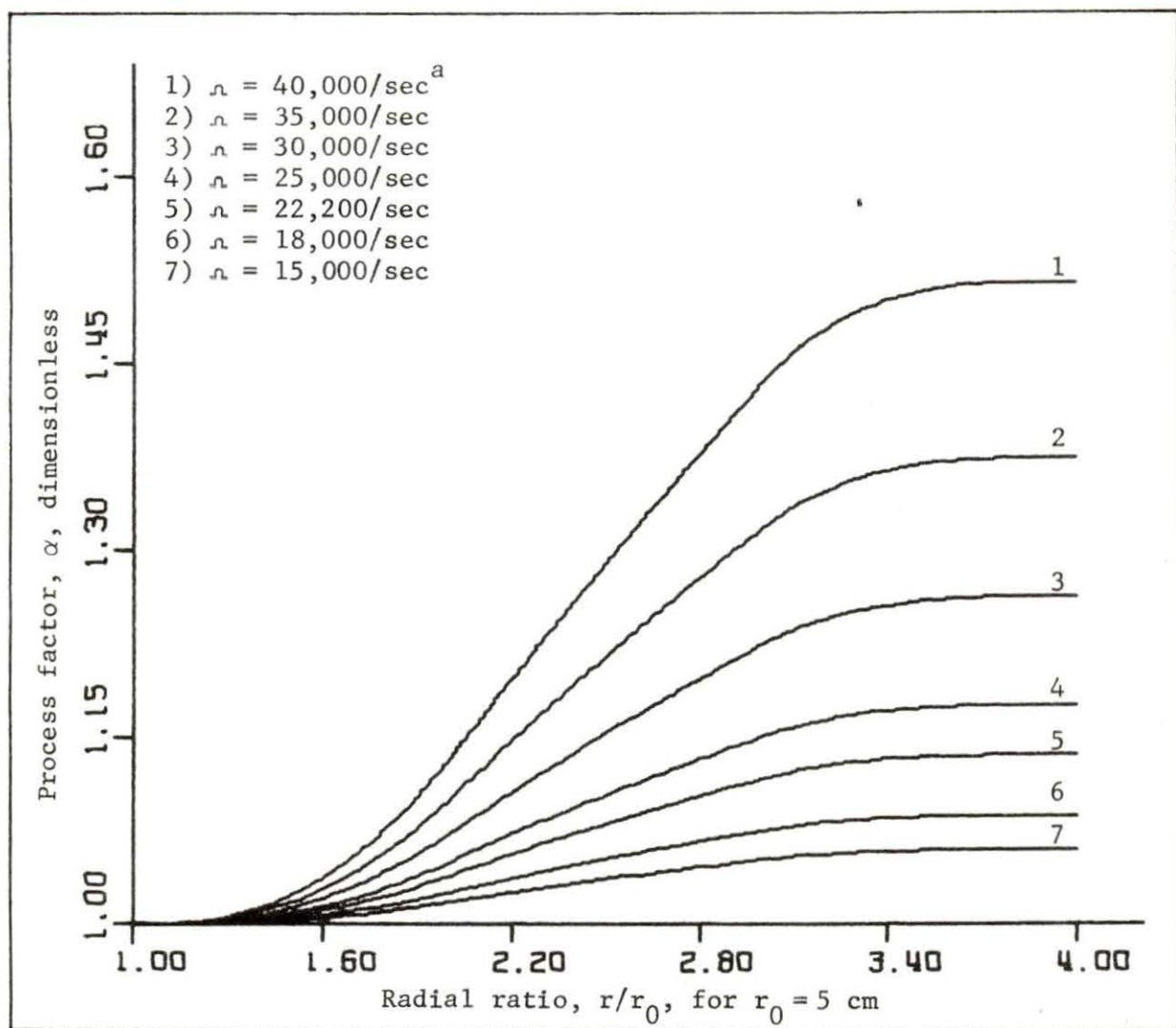
143      SUBROUTINE CONOMG(XI,RPI,Z,X,CONST)
144      COMMON PF,PP,ANG,V
145      PR=EXP(Z*(XI**2-RPI**2)/2.)
146      PP=EXP(X*(XI**2-RPI**2)/2.)
147      V=CONST*XI
148      ANG=CONST
149      RETURN
150      END
151      SUBROUTINE CONVEL(XI,RPI,Z,X,CONST)
152      COMMON PR,PP,ANG,V
153      PR=(XI/RPI)**(Z)
154      PP=(XI/RPI)**(X)
155      ANG=CONST/XI
156      V=CONST
157      RETURN
158      END

```

```
159      SUBROUTINE CONACC(XI,RPI,Z,X,CONST)
160      COMMON PR,PP,ANG,V
161      PR=EXP(Z*(1./RPI**2-1./XI**2)/2.)
162      PP=EXP(X*(1./RPI**2-1./XI**2)/2.)
163      ANG=CONST/XI**2
164      V=CONST/XI
165      RETURN
166      END
```

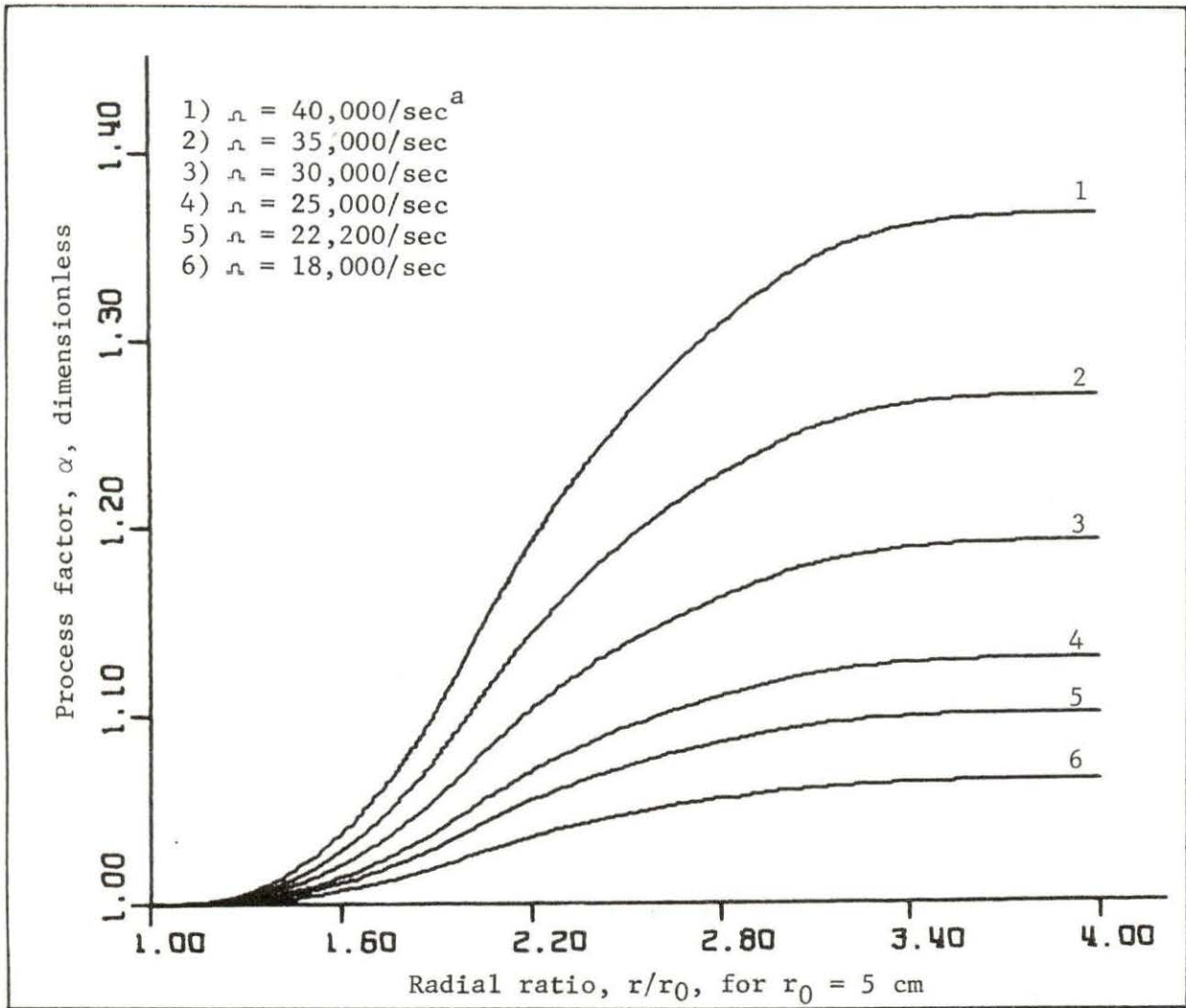
\$ENTRY

APPENDIX B. SUPPLEMENTAL FIGURES



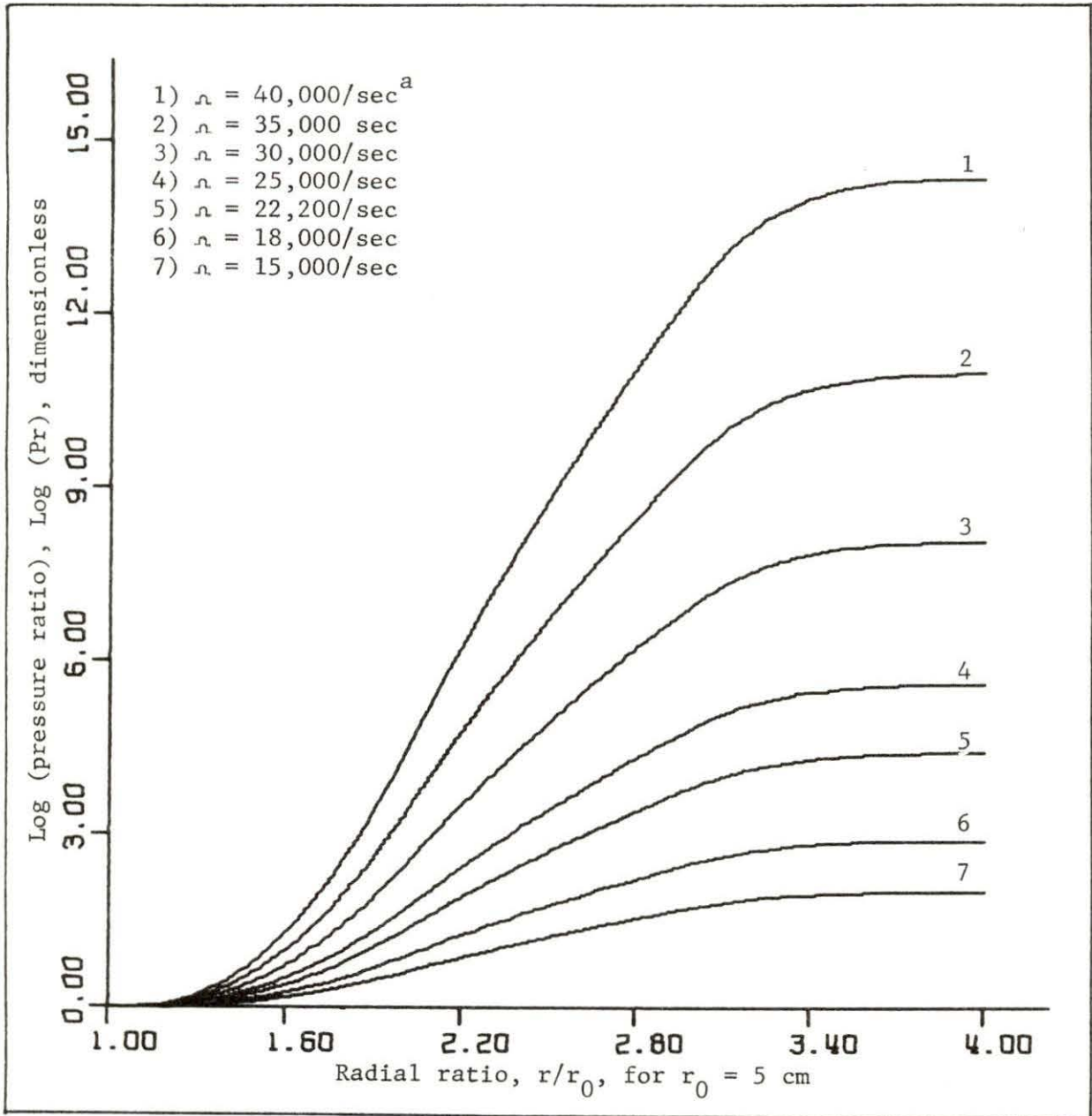
^a ω = angular velocity, temperature = 10,000 K.

Fig. B.1. Process factor as a function of angular velocity, where $\omega \times r = \text{const.}$



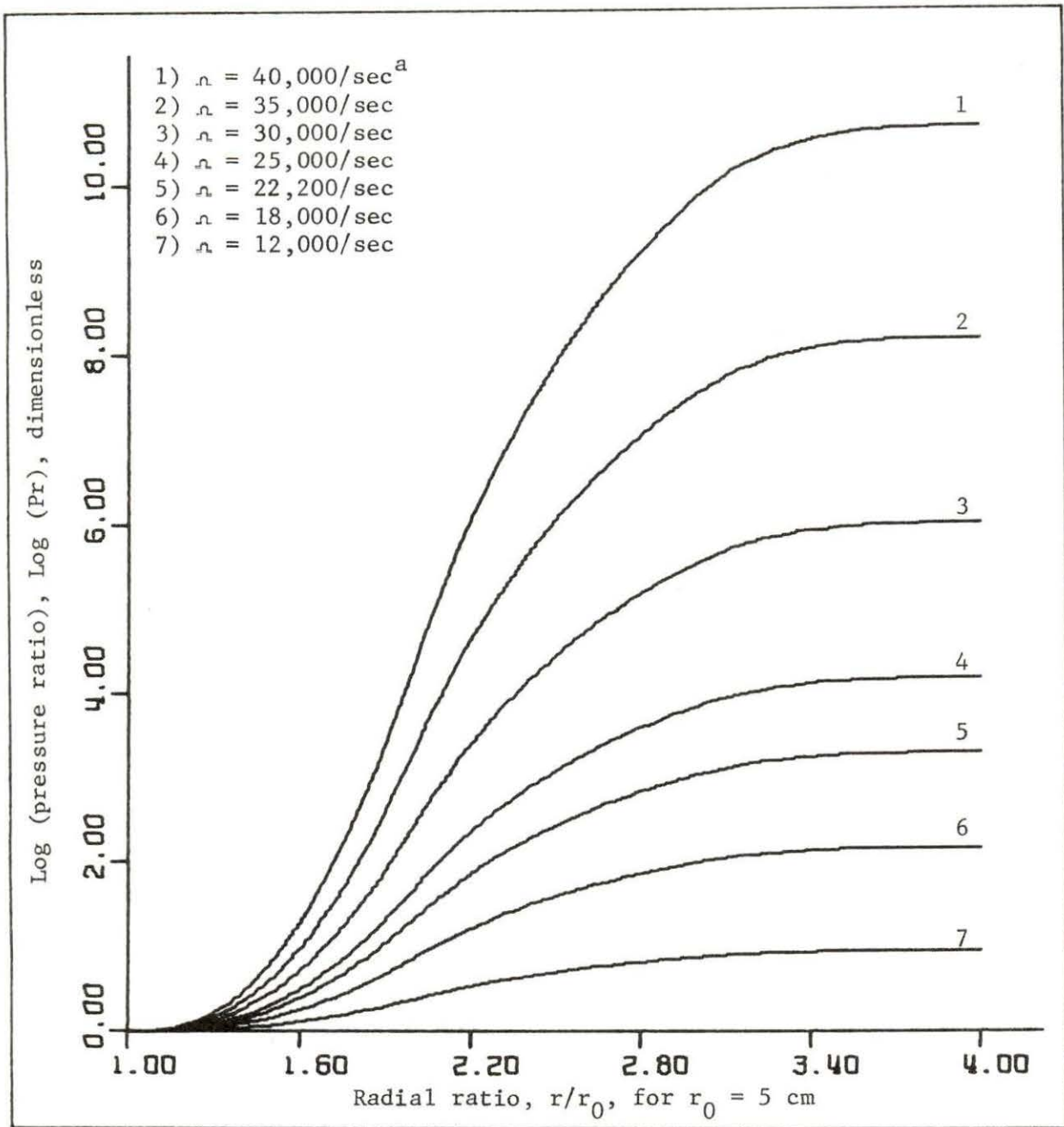
^a ω = angular velocity, temperature = 10,000 K.

Fig. B.2. Process factor as a function of angular velocity, where $\omega \times r^2 = \text{const.}$



^a $\omega =$ angular velocity, temperature = 10,000 K.

Fig. B.3. Pressure ratio as a function of angular velocity, where $\omega \times r = \text{const.}$



^a n = angular velocity, temperature = 10,000 K.

Fig. B.4. Pressure ratio as a function of angular velocity, where $n \times r^2 = \text{const.}$

Table B.1. Angular velocity distribution, $\omega \times \text{radius} = \text{constant}$ ^a

Rotational velocity, in sec^{-1}	Process factor, by region			Pressure ratio, by region		
	Inner	Plasma	Outer	Inner	Plasma	Outer
40,000	1.134	1.264	1.056	2.11×10^4	1.18×10^8	7.73×10^1
35,000	1.101	1.196	1.043	2.04×10^3	1.51×10^6	2.79×10^1
30,000	1.073	1.141	1.031	2.70×10^2	3.47×10^4	1.15×10^1
25,000	1.050	1.096	1.022	4.89×10^1	1.42×10^3	5.96×10^0
23,000	1.042	1.080	1.018	2.69×10^1	4.66×10^2	4.21×10^0
22,000 ^b	1.039	1.075	1.017	2.15×10^1	3.06×10^2	3.82×10^0
21,000	1.035	1.067	1.015	1.56×10^1	1.68×10^2	3.32×10^0
20,000	1.032	1.060	1.014	1.20×10^1	1.04×10^2	2.96×10^0
18,000	1.026	1.048	1.011	7.51×10^0	4.31×10^1	2.41×10^0
15,000	1.018	1.033	1.008	4.06×10^0	1.36×10^1	1.84×10^0
12,000	1.011	1.021	1.005	2.45×10^0	5.33×10^0	1.48×10^0
10,000	1.008	1.015	1.003	1.86×10^0	3.20×10^0	1.31×10^0

^aAssuming boundary walls at 5 and 20 cm, plasma edges at 10 and 15 cm.

^bCritical angular velocity at a radius of 0.1 m, temperature = 10,000 K.

Table B.2. Angular velocity distribution, $\omega \times (\text{radius})^2 = \text{constant}^a$

Angular velocity, in sec^{-1}	Process factor, by region			Pressure ratio, by region		
	Inner	Plasma	Outer	Inner	Plasma	Outer
40,000	1.134	1.174	1.025	2.11×10^4	3.78×10^5	6.91
35,000	1.101	1.131	1.019	2.04×10^3	1.71×10^4	4.39
30,000	1.073	1.094	1.014	2.70×10^2	1.29×10^3	2.96
25,000	1.050	1.065	1.010	4.89×10^1	1.44×10^2	2.13
23,000	1.042	1.054	1.008	2.69×10^1	6.73×10^1	1.89
22,000 ^b	1.039	1.051	1.008	2.15×10^1	5.05×10^1	1.81
21,000	1.035	1.045	1.007	1.56×10^1	3.34×10^1	1.70
20,000	1.032	1.041	1.006	1.20×10^1	2.41×10^1	1.62
18,000	1.026	1.033	1.005	7.51×10^0	1.32×10^1	1.48
15,000	1.018	1.023	1.003	4.06×10^0	5.99×10^0	1.31
12,000	1.011	1.014	1.002	2.45×10^0	3.14×10^0	1.19
10,000	1.008	1.010	1.002	1.86×10^0	2.22×10^0	1.13

^aAssuming boundary walls at 5 and 20 cm, plasma edges at 10 and 15 cm.

^bCritical angular velocity at a radius of 0.1 m, temperature = 10,000 K.

Table B.3. Temperature distribution, $\omega \times \text{radius} = \text{constant}$ ^a

Temperature	Process factor, by region			Pressure ratio, by region		
	Inner	Plasma	Outer	Inner	Plasma	Outer
15,000	1.026	1.049	1.011	7.72×10^0	4.54×10^1	2.44×10^0
10,000 ^b	1.039	1.075	1.017	2.15×10^1	3.06×10^2	3.82×10^0
9,000	1.043	1.083	1.019	3.02×10^1	5.79×10^2	4.43×10^0
8,000	1.049	1.094	1.021	4.62×10^1	1.28×10^3	5.33×10^0
7,000	1.057	1.108	1.024	7.99×10^1	2.72×10^3	6.78×10^0
6,000	1.066	1.128	1.028	1.66×10^2	1.39×10^4	9.32×10^0
5,000	1.080	1.155	1.034	4.61×10^2	9.38×10^4	1.46×10^1
4,000	1.101	1.198	1.043	2.14×10^3	1.64×10^6	2.89×10^1
3,000	1.138	1.272	1.058	2.75×10^4	1.94×10^8	8.68×10^1
2,500 ^c	1.167	1.335	1.070	2.12×10^5	8.80×10^9	2.12×10^2
2,000	1.213	1.434	1.088	4.56×10^6	2.70×10^{12}	8.09×10^2
1,500	1.294	1.618	1.119	7.56×10^8	3.76×10^{16}	7.54×10^3

^aAssuming boundary walls at 5 and 20 cm, and plasma edges at 10 and 15 cm, $v_c = 2200$ m/sec at 0.1 m.

^bTemperature assumed in the analysis by Lehnert [8].

^cTemperature assumed in the analysis by Okada et al. [13].

Table B.4. Temperature distribution, $\omega \times (\text{radius})^2 = \text{constant}^a$

Temperature	Process factor, by region			Pressure ratio, by region		
	Inner	Plasma	Outer	Inner	Plasma	Outer
15,000	1.026	1.034	1.005	7.72×10^0	1.37×10^1	1.49×10^0
10,000 ^b	1.039	1.051	1.008	2.15×10^1	5.05×10^1	1.81×10^0
9,000	1.044	1.056	1.008	3.02×10^1	7.81×10^1	1.94×10^0
8,000	1.050	1.064	1.009	4.62×10^1	1.35×10^2	2.10×10^0
7,000	1.057	1.073	1.011	7.99×10^1	2.71×10^2	2.34×10^0
6,000	1.066	1.086	1.012	1.66×10^2	6.90×10^2	2.70×10^0
5,000	1.080	1.104	1.015	4.61×10^2	2.55×10^3	3.29×10^0
4,000	1.101	1.132	1.019	2.14×10^3	1.81×10^4	4.43×10^0
3,000	1.138	1.179	1.025	2.75×10^4	4.75×10^5	7.27×10^0
2,500 ^c	1.167	1.219	1.030	2.12×10^5	6.50×10^6	1.08×10^1
2,000	1.213	1.280	1.038	4.56×10^6	3.28×10^8	1.96×10^1
1,500	1.294	1.390	1.051	7.56×10^8	2.26×10^{12}	5.29×10^1

^aAssuming boundary walls at 5 and 20 cm, and plasma edges at 10 and 15 cm, $v_c = 2200$ m/sec at 0.1 m.

^bTemperature assumed in the analysis by Lehnert [8].

^cTemperature assumed in the analysis by Okada et al. [13].